995

A157616

ADA157616

R and D CENTER

LABORATORY

TECHNICAL REPORT

NO. 13100

Improvement in the Fatigue Behavior of Tank Track Pins

by J.F. Wallace & A.M. Said
Case Western Reserve University
Department of Metlal[illegible]gy & Mat'l Sci.
10900 Euclid Avenue
Cleveland, Ohio 44106

20020725089

U.S. ARMY TANK-AUTOMOTIVE COMMAND
RESEARCH AND DEVELOPMENT CENTER
Warre[illegible], Michigan 48090

AN-46869

CASE WESTERN RESERVE UNIVERSITY
University Circle
10900 Euclid Avenue
Cleveland, Ohio 44106
JOHN F. WALLACE
Department of Metallurgy & Materials Science

1-Kg 1

Commander
US Army Tank-Automotive Command
ATTN: AMSTA-TSL (Technical Library
Warren, MI 48397-5000

15

14 OH 4-84-849 UNITED PARC

REPORT DOCUMENTATION PAGE

1a. REPORT SECURITY CLASSIFICATION: Unclassified	1b. RESTRICTIVE MARKINGS: None
2a. SECURITY CLASSIFICATION AUTHORITY	3. DISTRIBUTION/AVAILABILITY OF REPORT: Approved for public release; distribution unlimited.
2b. DECLASSIFICATION/DOWNGRADING SCHEDULE	
4. PERFORMING ORGANIZATION REPORT NUMBER(S): 13100	5. MONITORING ORGANIZATION REPORT NUMBER(S)
6a. NAME OF PERFORMING ORGANIZATION: Case Western Reserve University; 6b. OFFICE SYMBOL (If applicable)	7a. NAME OF MONITORING ORGANIZATION: U. S. Army Tank Automotive Command
6c. ADDRESS (City, State, and ZIP Code): 10900 Euclid Avenue, Cleveland, Ohio 44108	7b. ADDRESS (City, State, and ZIP Code): Warren, MI 48397-5000
8a. NAME OF FUNDING/SPONSORING ORGANIZATION: U. S. Army Tank Automotive; 8b. OFFICE SYMBOL (If applicable): AMSTA-RCKT	9. PROCUREMENT INSTRUMENT IDENTIFICATION NUMBER: DAAE07-83-K-R006
8c. ADDRESS (City, State, and ZIP Code): Warren, MI 48397-5000	10. SOURCE OF FUNDING NUMBERS: PROGRAM ELEMENT NO. / PROJECT NO. / TASK NO. / WORK UNIT ACCESSION NO.

11. TITLE (Include Security Classification)

"Improvement in the Fatigue Behavior of Tank Track Pins"

12. PERSONAL AUTHOR(S)

13a. TYPE OF REPORT	13b. TIME COVERED	14. DATE OF REPORT (Year, Month, Day)	15. PAGE COUNT
	FROM Mar 1983 TO Aug 1985	Aug. 1985	92

16. SUPPLEMENTARY NOTATION

17. COSATI CODES			18. SUBJECT TERMS (Continue on reverse if necessary and identify by block number)
FIELD	GROUP	SUB-GROUP	

19. ABSTRACT (Continue on reverse if necessary and identify by block number)

This investigation is aimed at improving the fatigue behavior of tank track pins through the use of better processing methods and materials. Five different compositions of steels investigated: SAE 8650H, 4340,4140, 8620 and 1045. These were subjected to the following treatments: induction hardening, stress shot peening, nitriding and carburizing. All steels except 1045, received final treatment of shot peening. Tension-tension bending fatigue tests were conducted on these pins to determine the S-N curve of each type of steel and the result compared with the data on the regular production tank tack pins obtained in another investigation.

Stress shot peened 8650H pins have the highest residual compressive stress of -175 ksi on the surface and demonstrate the best fatigue limit of 198 ksi. The induction hardened, nitrided and carburized 4340, 4140 and 8620 steel pins, which have been

20. DISTRIBUTION/AVAILABILITY OF ABSTRACT	21. ABSTRACT SECURITY CLASSIFICATION	
☒ UNCLASSIFIED/UNLIMITED ☐ SAME AS RPT. ☐ DTIC USERS	Unclassified	
22a. NAME OF RESPONSIBLE INDIVIDUAL: John F. Wallace	22b. TELEPHONE (Include Area Code): (216) 368-4222	22c. OFFICE SYMBOL: Met. & Mat'l. Sci.

19. (Continued) ABSTRACT

shot peened, have a surface hardness range of Rc 58 -62 and shown an equal level of compressive residual stress of about -110 ksi on the surface. Carburized 8620 pins demonstrate the second highest fatigue limit of 175 ksi followed in turn by induction hardened and stress shot peened 4340, induction hardened and nitrided 4140 and carburized 1045 with the lowest fatigue strength.

TABLE OF CONTENTS

TABLE OF CONTENTS (Continued)

LIST OF ILLUSTRATIONS

LIST OF ILLUSTRATIONS (Continued)

LIST OF ILLUSTRATIONS (Continued)

THIS PAGE INTENTIONALLY LEFT BLANK

LIST OF TABLES

THIS PAGE INTENTIONALLY LEFT BLANK

1.0. INTRODUCTION

This investigation is directed toward enhancing the fatigue properties of tank track pins in service through better processing and steel selections. The tank track pins have been observed to fail in fatigue as a result of high bending stress conditions and frequent shock loading during certain maneuvering of the tank. In addition, the surface of the pins is subjected to wear which could produce stress concentration or worn areas that can service as initiation sites for fatigue failures.

2.0. OBJECTIVES

At the present time, the tank track pins, per Figure 2-1, are being produced from SAE8650H alloy steel. The pins are machined to about a 1.25-inch diameter, 28-inch length with a 0.5 inch central hole drilled the entire length. The outer diameter of the pin has a 63 microinch finish and the inner diameter a 125-microinch finish. One 1.81-inch long flat with a maximum depth of 0.169-inch is machined starting at 0.31-inch from either end. After machining, the bar is quenched and tempered to a Rockwell C hardness of 55 to 60 to a depth of at least 0.060 inch. No more than 0.005 inch partial decarburization is permitted. The final operation, after straightening if needed, is shot peening to about a 0.012C Almen strip with 390 or 460 steel shots. It is apparent from this processing method that many techniques are being employed to enhance the fatigue resistance of the steel pins. The hardness and carbon content were selected to provide good fatigue resistance. The surfaces are induction hardened to provide both the higher strength and compressive stresses that improve fatigue properties. Finally, shot peening is employed under specified conditions that are known to increase the fatigue resistance considerably. Despite the use of this steel, heat treatment, surface hardening, and shot peening, fatigue failures continue to occur.

Since these fatigue failures start at the surfaces of the pins, improved surface treatments over those now employed could provide better fatigue resistance surface and hence increased fatigue strength of the pins. Three of these surface treatments undertaken in this investigation are gas carburizing, gas nitriding, and stress shot peening.

Gas carburizing is a process in which a high carbon concentration is introduced into the steel surface for absorption and diffusion into the low carbon steel to provide a hardened case up to 0.08 inch at the surface with a hardness up to Rockwell C 67. The introduction of a high carbon level at the surface delays the austenite-martensite transformation in the case so that it occurs relatively slowly. The resulting volume expansion in the case is resisted by the already hardened and expanded core, placing the case in compression. Finishing the carburized surface with shot peening would result in higher surface compressive residual stress and improved fatigue life [1,2].

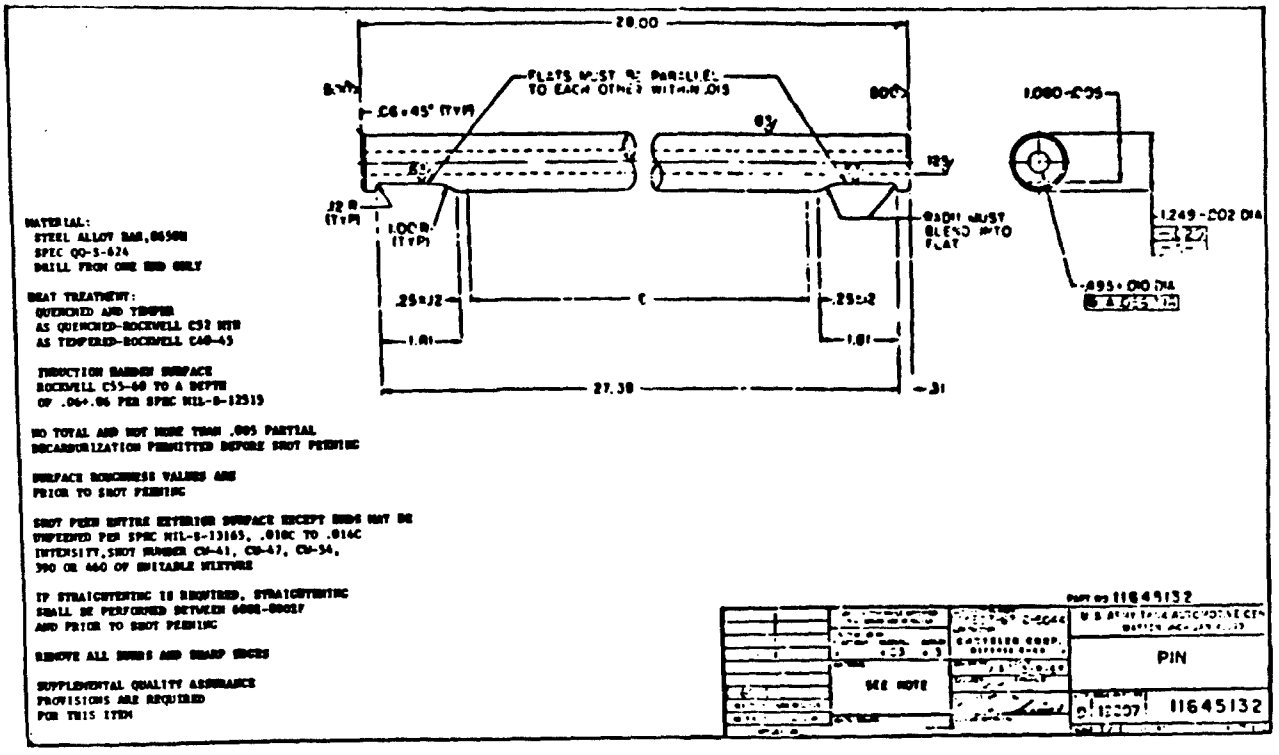

Figure 2.1. Regular Production (As Received) Tank Track Pin

Nitriding has been shown to improve the fatigue life of many steel components . In gas nitriding, nitrogen is introduced into the surface of the steel by holding at a suitable temperature (925-1050°F). A thin nitride layer ranging from 0.001 to 0.005 inch formed on the surface has a very high hardness (may exceed Rockwell C 72) and wear resistance. As in the case of carburizing, the nitride forms during the last stage of transformation and the resulting increase in volume induces compressive stresses on the surface. Shot peening the nitrided steel will result in even higher surface residual compressive stress and fatigue limit [3].

Stress shot peening is a more recent development of shot peening [4,5]. It consists of shot peening the part while it is being statically stressed in the same sense as the stress to be applied in service. This process is particularly suitable for parts subjected to repeated unidirectional bending or torsion stresses, such as leaf springs, coil springs and as well as tank track pins. The peening is conducted in accordance with the normal practice except for the application of a tensile static stress during the peening process. After peening the static stress is removed and the process is complete. The increase in fatigue strength resulting from stress shot peening exceeds the improvement from conventional shot peening [6]. This improvement is attributed to the higher residual compressive stress at the surface obtained by this process than that obtained by conventional shot peening [7].

In this investigation, tank track pins made of five different kinds of steels were studied. They are 8650H, 4340, 4140, 8620, and 1045 steels. These different steels were subjected to various heat and surface treatments which included induction hardening, carburizing, nitriding, shot peening, and stress shot peening. Some specimens of 4340 and 4140 steels are processed in a similar manner as that of the original 8650H tank track pins which involves quenching and tempering, induction hardening, and shot peening. The effect of different steels, heat treatments, surface treatments, microstructure, surface residual stresses, and the steel cleanliness on the fatigue strength of the pins are examined and the results compared to those of the original tank track pins.

3.0. RECOMMENDATIONS

The best fatigue properties attained on these tank track pins was in the stress shot peened condition. The improvement in fatigue life in this condition was so great that pilot trials of stress shot peened pins in tanks are indicated to determine the service behavior of pins processed in this manner. If stress shot peened pins prove to provide superior service behavior consideration should be given to changing the processing production method of tank track pins to this process.

4.0. CONCLUSIONS

Stress shot peening produces the highest compressive residual stress on the surface and provides the highest endurance limit of the tank track pins. Regardless of the pre-shot peening conditions of the various steels, the surface residual stress level after peening are about the same at -110 ksi within a small range of surface hardness between Rc 58-62. With an equal surface compressive residual stress level of about -110 ksi, the highest surface and core hardness of carburized 8620 steel pin provides the highest endurance limit. The apparent high ductility of 4340 steel pins produces the best fatigue strength of the induction hardened pins.

5.0. DISCUSSION

5.1.1. Literature Review

Fatigue failure accounts for the vast majority of service failures in machine components. It has been often stated that fatigue failures account for 90 percent of total service failure due to mechanical causes . Metals that were known to be ductile were observed to fail in what appeared to a "brittle" manner when subjected to repeated loads that were considered to be "safe". For iron and steels having ultimate tensile strengths up to 200 ksi, fatigue failures occur at maximum altenating stresses ranging from 0.35 to 0.6 of the tensile strength [9] . Below a certain stress level known as the endurance limit, the metal can supposedly endure an infinite number of cycles without failure. However, for nonferrous metals such as Al, Ni and their alloys, such definite endurance limits do not exist. The explanation for this was stated by Rally and Sinclair [10] who found that metals which undergo strain aging have an S-N curve with a sharp knee and a well-defined fatigue limit. As the tendency for strain aging decreases, the S-N curve flattened out and the knee occurred at a larger number of cycles. Lipsitt and Horne [11] also found similar results and proposed that the fatigue limit represents the stress at which a balance occurs between fatigue damage and localized strengthening due to strain aging.

Many mechanisms have been proposed to explain the fatigue phenomena [12,15] . In general, the dominant features of fatigue phenomena comprise of local plastic strains, cyclic hardening and softening, crack initiation and growth and final fracture. In the primary stage, local plastic and strain hardening occurs at small weak regions which may be areas of favorable slip orientation or areas of high stress concentration because of metallurgical notches such as inclusions. In the next stage, as shear stresses overcome the shear flow strength of the metal, to-and-fro flow or slips lead to fatigue crack initiation in which visible fatigue cracks are produced [16] . The third stage involves the growth of these cracks to a critical length at which final fracture occurs.

The many factors that affect fatigue such as the materials and their properties, heat treatment, surface condition, residual stresses, microstructure, cleanliness, type of loading, and environment, make fatigue a complex subject and an active area of investigations. A machine component that fails in fatigue is therefore unique to a particular set of circumstances between the above factors. Laboratory tests must therefore be conducted in as similar condition as possible to those subjected to the part during service in order to determine accurately the fatigue strength of the part.

Fatigue may occur as a result of axial, bending, contact, torsional, or a combination of any of these loads. Regardless of the method of loading, a stress system develops comprised of principal and shear stresses. Shear stresses overcoming the shear flow strength of the material cause flow, and to-and-fro flow is a necessary requisite to fatigue crack initiation [16]. When fatigue occurs, the material has experienced fluctuating loads and accompanying shear stresses which have caused repeated flow of the material at the failure-origin area [17]. The material has to resist the explicit stresses resulting from the forces being applied at the critical locations. Hence the material must exhibit strengths that are directly related to the stress system set up by the applied forces that are compatible with the stresses. Important concepts related to this are the brittle and and ductile concepts. Materials with a large fracture/flow strength ratio are thought of being ductile, whereas materials with low fracture/flow strength ratios (approaching 1) are thought of being brittle [18]. Brittle or ductile behavior can be influenced greatly by the principal-stress/shear-stress ratio of the stress system being applied. Ductile materials and ductile load systems provide better resistance to fatigue presumably, in part, at least, because they are better able to accommodate flaws [18].

Most fatigue failures originate on the surfaces of the components rather than below the surfaces. Exceptions are when metallurgical defects are present below the surface or the gradient strength is insufficient such as in tensile-tensile fatigue stressing. Geometric stress concentrations arising from machining and handling defects, designed notches such as keyways, slots and holes, decarburization and corrosion or other environmental conditions, are highest at the surface and make the surface more susceptible to failure. In addition, the loading condition such as bending and torsion create stresses that are maximum at the outer dimensions. Numerous studies indicate that the fatigue strength of many steels decreases with increasing surface roughness or discontinuities [19,27].

Surface residual stress induced in a component as a result of cold working or heat treatment can be beneficial or detrimental to the fatigue life because it is additive to the stresses resulting from external applied loads [28] Thus a part loaded in bending or torsion with tensile residual stresses at the surface, will possess poor fatigue strength. However, if a compressive residual stress is present [7], it will act to diminish the applied tensile

stress and increase the endurance limit. Such processes that produce tensile residual stresses at the surface are decarburization [29,30], grinding and various electroprocesses such as electro discharge machining. Processes that produce compressive residual stresses at the surface and increased fatigue strength are carburizing [1,2], nitriding [3], flame hardening, induction hardening [31] and cold working processes such as polishing, cold rolling, and shot peening [7]. Compressive residual stresses arising from heat treatments are brought about by nonhomogeneous transformations in a part. For example, the austenite to martensite transformation in steel results in an appreciable increase in volume. When this transformation occurs in a thin layer on the surface, as in the case of flame hardening and induction hardening, the increase in surface volume puts the surface into compression. In carburizing and nitriding, the transformations of martensite and nitride in the case respectively, occur in the last stage of a series of transformations. The resulting increase in volume in the case thus puts the surface into compression. Cold working, such as shot peening of the surface of a component, causes plastic deformation and elongation of a thin layer of material on the surface [6]. This nonhomogeneous plastic deformation results in an increase in surface length and hence compressive residual stresses.

Shot peening is a cold working process in which a shower of hard shot, usually high carbon steel, is blasted or thrown against the surface of the component. This process is considered to be one of the most convenient and effective surface treatment methods that can be applied to improve the fatigue strength. The increase in fatigue strength can be attributed to two reasons; the surface layers are hardened; and compressive residual stresses are obtained in these layers [32]. The latter are more potent in improving fatigue properties than the work hardening effect [7,19]. The maximum magnitude of compressive residual stress produced at or near the surface of peened steel varies from about 110,000 psi for a 150,000 psi tensile strength to 132,000 psi at a 250,000 psi tensile strength level [33]. The depth of residual stress depends on the hardness and ductility of the peened metal, the state of strain at the time of peening and the characteristics of the shot and shot stream [33]. These variables are determined by: the material, size, hardness, and uniformity of sphericity of the shot, the angle of impact of the shot stream, the shot velocity, and the peening time. The degree of coverage is determined by the number of impacts per unit area. Increasing the number of impacts per unit area provides a more uniform depth of cold work [34].

The microstructure of the component produced by heat treatment has a significant effect on the fatigue strength. For steels, a completely tempered martensitic microstucture provides the best fatigue limits. Even the presence of a small amount of nonmartensitic products poses a deleterious effect on the fatigue strength. If the surface is less than 100 percent martensite, the endurance limit decreases. This decrease is relatively sharp at the 95 percent martensite and more gradual between 95 percent and 85

percent martensite [35]. Below 85 percent martensite, the endurance limit is little affected by microstructure. The cleanliness of the steel also exerts a significant effect on the fatigue strength. It has been shown that reduced inclusion counts improve the fatigue life of steel components [36,37]. The effect of smaller size spherical inclusions has been demonstrated to improve the fatigue life of steels [38].

5.2. MATERIALS AND PROCEDURE

5.2.1. Materials

This investigation involved the processing of five different types of steel. These different types of compositions, the nominal ranges of which are shown in Table 5-1., were selected to determine the effect of different steels and processing on the fatigue behavior of tank track pins. The 8650H steel was obtained as regular production tank track pins [39] completely heat treated and processed in accordance with part number 11645132 as shown in Figure 2-1. This figure indicates that the pins are to be liquid quenched and tempered to provide a core harness of Rc 40 - 45. After this treatment the outer surface of the pin is to be induction hardened to provide a case depth of 0.06 inch + 0.06 inch with a hardness range of Rockwell C 55 - 60. The other steels, AISI 4340, 4140, 8620 and 1045, were selected to provide a range of methods of obtaining different types of surface hardness. The 8620 steel was processed by a conventional carburizing to obtain a surface hardness of Rc 60 -62 and an effective case depth of 0.079 inch. The 4140 steel was given a two-stage gas nitriding treatment. The first stage was conducted at 980°F for 8 hours (ammonia dissociation rate 30 percent) and the second stage at 1050°F for 64 hours (ammonia dissociation rate of 80 percent) to provide a hardness of Rc 60 - 62 at the surface and a nitrided case of 0.02 inch plus 0.004 inch depth. The 4340 steel was processed in a similar manner to the regular production 8650H steel which involved liquid quenching and tempering followed by induction hardening to provide a surface hardness of Rc 55 - 60.

The 1045 steel bars were processed by a special treatment that was designed to provide a very high compressive residual stress on the surface. This technique is described in reference [40] and consists of water quenching and tempering at 400°F. However, difficulty was experienced with a decarburized surface layer and the desired hardness was not obtained at the surface with this treatment. This made it necessary for the bars to be reprocessed with a conventional gas carburizing treatment to provide a surface hardness of Rc 60 - 62 and an effective case depth of 0.079 inch.

Most of these pins of different compositions and processing methods were finished by shot peening the outer surface. The standard production pins were shot peened per specification MIL-S-13165B [41]. The same type of peening was also employed for the 4340, 8620 carburized and 4140 nitrided.

Table 5-1. Composition Ranges of Steels Investigated

Material	C	Mn	Si	Cr	Ni	Mo	Pmax	Smax
8650H	0.47-0.54	0.7-1.05	0.15-0.3	0.35-0.65	0.35-0.7	0.15-0.7	0.035	0.04
4340	0.38-0.43	0.6-0.8	0.15-0.3	0.7-0.9	1.65-2.0	0.2-0.3	0.035	0.04
4140	0.38-0.43	0.75-1.0	0.1-0.3	0.8-1.1	-	0.15.0.25	0.035	0.04
8620	0.18-0.23	0.7-0.9	0.15-0.3	0.4-0.6	0.4-0.7	0.15-0.25	0.035	0.04
1045	0.43-0.5	0.6-0.9	-	-	-	-	0.035	0.05

Metals Handbook, 9th Edition, Vol. 1, ASM, Metals Park, Ohio 1978, pp. 125-130.

Whereas the standard pins were shot peened with shot number 390 or 460 to a 0.010 - 0.014C Almen intensity, the 4340, 4140 and 8620 were shot peened with 330 shot to a 0.011C Almen intensity. The 1045 carburized steels were not shot peened. A summary of the processing techniques used on each type of pin is listed in Table 5-2.

The production pins were purchased from Blairsville Machine Products, Pennsylvania to Part No. 11645132 as shown in Figure 2-1. The others, 4340, 4140, 8620 and 1045 steels were purchased in the form of hot rolled round bar stock with nominal diameter of 13 inches. These bars were cut to 29 inches lengths, machined to a 1.270 inch outer diameter, the central hole drilled through the entire length from one end to a 0.6 inch bore and cut to a final length of 14 inches. Heat treatment of quenching and tempering was conducted to provide a core hardness of Rc 40 -45 and the bars were finished ground to a 1.25 inch outer diameter. The various treatments of carburizing, nitriding, and shot peening were then employed on the pins.

5.2.2. Stress Shot Peening

Twelve test pins of 8650H and 4340 steels were stress shot peened before fatigue testing. The 8650H pins were obtained as regular production pins which had been liquid quenched and tempered and induction hardened per drawing of Part No. 11645132 but not shot peened. The flat ends of the pins were removed and the pins were cut to 11 inches lengths. After this, both ends were thread ground as shown in Figure 5-1 Prior to heat treatment, the 4340 pins in 14-inch lengths were first threaded on both ends as shown in Figure 5-2. They were then processed in a similar manner as the production pins. This involved liquid quenching and tempering to a core hardness of Rc 40 - 45 and induction hardened to provide a surface hardness of Rc 55 - 60 with a case depth of 0.06 inch. Two electrical strain gages, positioned 180 percent to each other were then mounted on the mid length of each pin.

The stress shot peening was conducted in a specially designed fixture illustrated in Figure 5-3 . A test pin was loaded in the fixture by screwing the threaded ends into two pin holders in the top and bottom plates of the fixture. The strain gages were then wired to a Baldwin Lima-Hamilton Model 120A portable strain indicator. Compensating strain gages were incorporated in the circuit to avoid any temperature effect on strain readings. A tensile load was applied to the pin through two 20-ton hydraulic jacks using a hand pump. From the strain readings, it was possible to determine the exact tensile stress induced in the pin. A hydraulic pump pressure of 8,000 psi was selected. This was equivalent to 89,700 lbs. load and a tensile stress of 87 ksi in the pin. When a steady pump pressure of 8000 psi was reached, the strain gages were removed and shot peening was conducted manually on the entire surface of the pin. Hard shot steel size 330 was used with a peening intensity of 0.011C, as shown in Figure 5-4. Care was taken to ensure that the pump pressure was maintained at 8,000 psi throughout the en-

Table 5-2. Summary of the Processing of Specimens

Group	Material	Heat Treatment	Shot Peening Treatment
1	SAE8650H	Quenched and tempered to Rc 40-45 core hardness, induction hardened to .06 ±.06 in. depth with Rc 55-60 surface hardness.	Stress shot peened after heat treatment
2	SAE4340	Austenized to 1550°F, oil quenched, tempered at 600°F, induction hardened to 0.125 in. case depth with Rc 55-60 surface hardness.	Stress shot peened after heat treatment
3	SAE4340	same as in (2)	Regular shot peened after heat treatment

Table 5-2. Summary of the Processing of Specimens (Continued)

4	SAE4140	a) same as in (2) b) 2-stage gas nitrided; First stage at 980°F for 8 hours with ammonia dissociation rate of 30%; Second stage at 1050°F for 64 hours with ammonia dissociation rate of 80%. Effective hardening depth 0.02 in. and surface hardness Rc 60-62.	Regular shot peened after heat treatment
5	SAE4140	a) same as in 4a	same as in (4)
6	SAE8620	Gas carburized at 1700°F with 0.9 carbon level, furnace cooled, austenized at 1550°F, oil quenched and tempered at 300°F to to surface hardness Rc 60-62	Regular shot peened after heat treatment
7	SAE1045	Gas carburized at 1100°F with 0.9 carbon level, furnace cooled, austenized at 1550°F, oil quenched and tempered at 300°F to Rc 60-62 surface hardness	Not shot peened

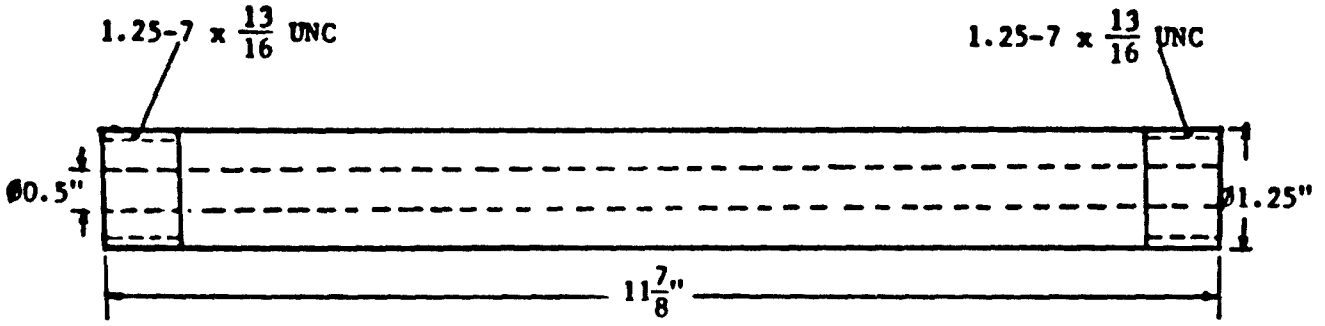

Figure 5-1. 8650H Fatigue Test Bar For Stress Shot Peening

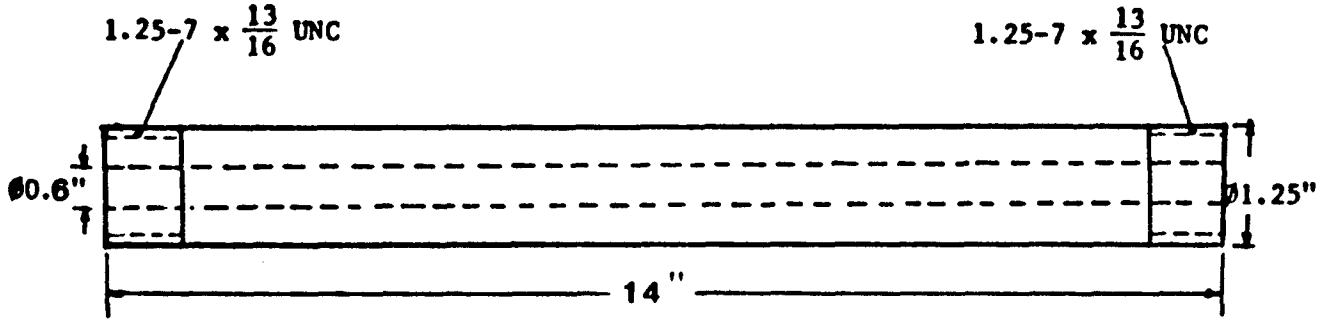

Figure 5-2. 4340 Fatigue Test Bar For Stress Shot Peening

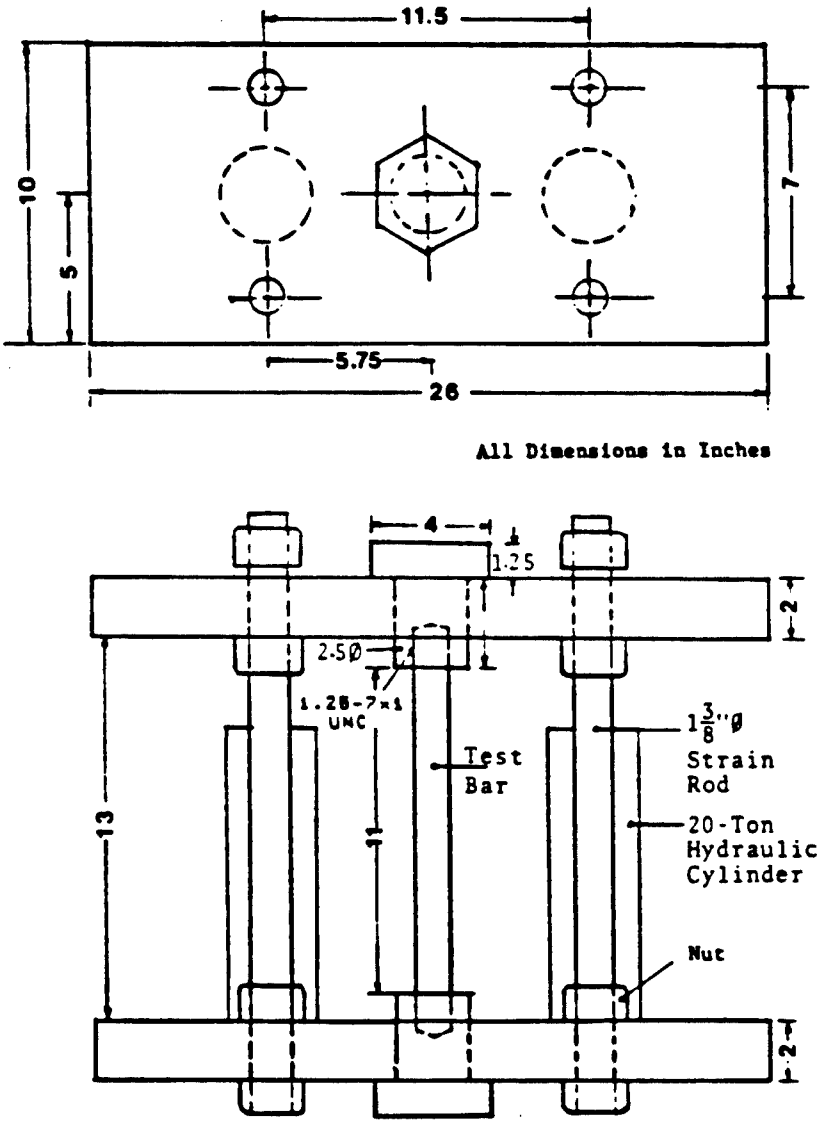

Figure 5-3. Stress Shot Peening Fixture

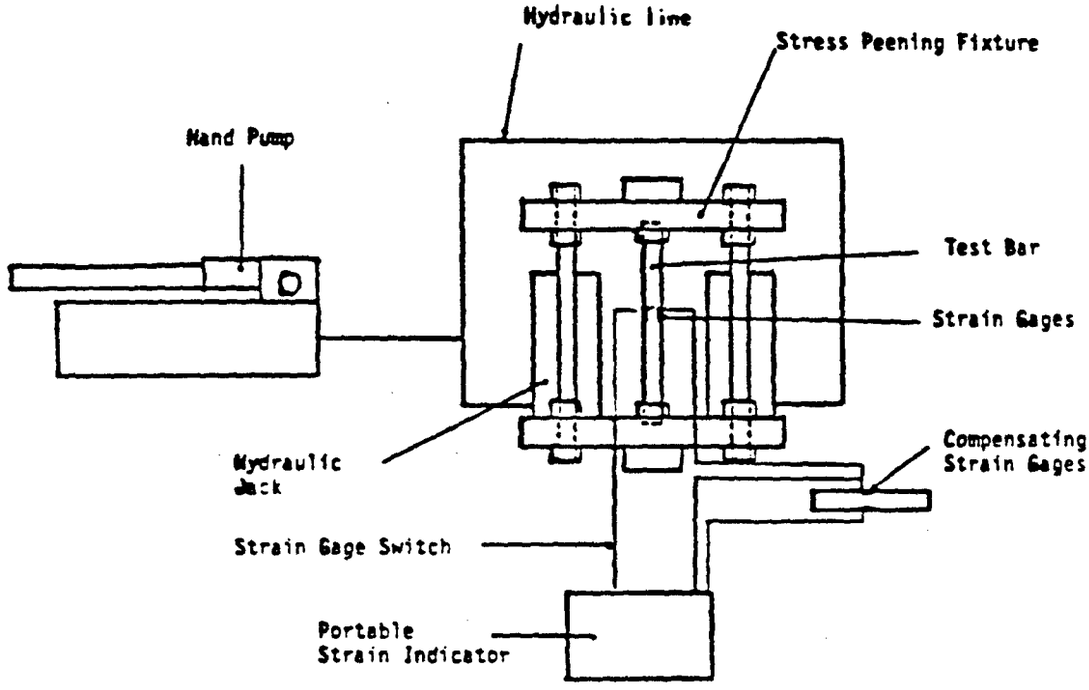

Figure 5-4. Equipment Set-up For Stress Shot Peening

tire peening process. When shot peening was completed, the pump pressure was released and the pin removed from the fixture. The entire procedure was repeated on the remaining pins.

5.2.3. Fatigue Testing

Fatigue testing on all specimens were conducted on an MTS machine using the special fixture shown in Figure 5-5. The specimen was subjected to a four point bending load with an outer span of 10 inches and an inner span of 0.825 inch as indicated in Figure 5.6. All specimens were 14 inches in length except for 8650H steel which were 11 inches in length. The bars were stressed in bending fatigue with a small tension to high tension at a 10 Hz frequency.

The maximum bending stress on the surface is computed from

$$\sigma_{max} = \frac{M \cdot y}{I}$$

where

M = maximum bending moment (in.lb)
y = distance from neutral axis (in)
I = area moment of inertia (in^4).

Hence,

$$\sigma_{max} = \frac{8P(L-l)D}{(D^4-d^4)}$$

where

P = applied load (lbs)
D = outer diameter of specimen (in)
d = inner diameter of specimen (in)
L = outer span (in)
l = inner span (in)

For L=10 in., l=0.825 in., D=1.25 in., d=0.5 in.,

$$\sigma_{max} = 12.274P$$

Stress on the pin was measured on the MTS machine. Actual bending stress was measured by mounting a temperature compensated strain gage on the mid span position of the pin. Bending loads were applied at 1,000 lbs. intervals and the strain gage measurements were used to determine the measured bending stress. These stresses were compared to the calculated values shown above.

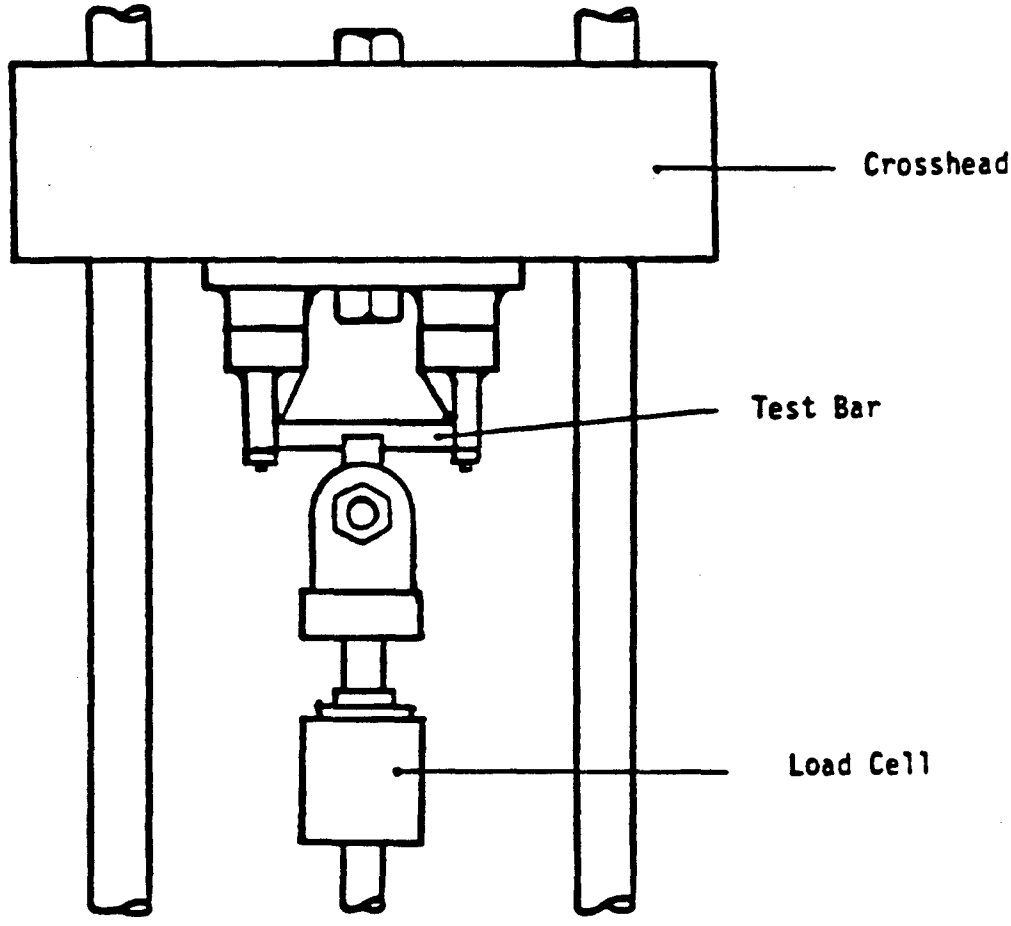

Figure 5-5. Fatigue Test Set Up On An MTS Machine.

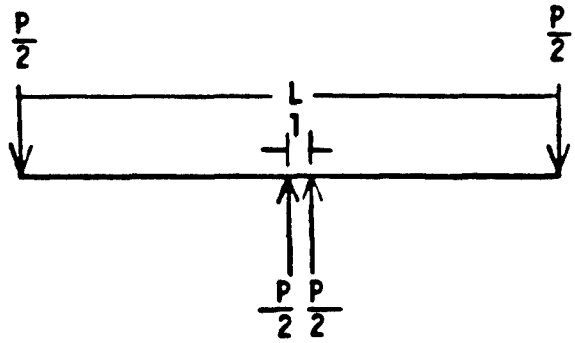

Figure 5-6. Four-Point Bending Load on Test Bar.

5.2.4. Metallographic Testing

Fatigue fracture surfaces of all specimens in each group were studied to determine the failure mode of each type of pin. The fracture surfaces were photographed to show the fatigue failure origins and the profiles of the fractured surfaces. Some specimens with fatigue cracks arrested before total fracture occurred were sectioned through planes perpendicular to the transverse cross section of the pins. These surfaces were ground and polished to reveal the nature of the fatigue cracks. Metallographic specimens of each type of pin were also prepared for microstructural studies. Specimens were obtained from portions cut at two inches from the fracture surfaces of fatigue bars and the plane parallel to the longitudinal cross-section of the pins were ground and polished. A 2 percent nital etchant was used to reveal the microstructures.

5.2.5. Microhardness Testing

Microhardness measurements on the cross section of each type of pin were conducted using a Leitz Wetzler Miniload Hardness Tester Specimens for microhardness measurement were taken from portions that were cut 2 inches from fracture surfaces of fatigue pins and the plane parallel to the longitudinal cross-section of the pins were ground and polished. Diamond Pyramid Hardness (Vickers) measurements taken at about 0.01 inch intervals in the hardened case and about 0.05 inch intervals in the core were made across the cross-section using a 2,000g load. A Rockwell hardness test was taken at about 0.1 inch intervals across the cross-section of the same specimen and the results compared to the microhardness readings.

5.2.6. Residual Stress Measurement

Surface residual stress measurements were performed using X-ray method on a Fastress machine. This was conducted at American Analytical Corporation, Grafton, Ohio. Fastress system, was developed by General Motors Corp. It is an automatic X-ray residual stress analyzer which presents data directly on a calibrated strip chart recorder in psi within seconds. Residual stress determination of soft steel can be performed in 10 seconds, hardened steel in 30 seconds and aluminum in less than 30 seconds [42]. The instrument has two X-ray sources, 60° apart, which irradiate the same area of the sample at the same time. The detected output drives two servomechanisms to find two points of equal corrected intensity on each peak of reflected X-ray energy. Differences between peaks indicates the stress which is automatically recorded directly on a strip chart. By moving the sample past the X-ray beams or by transversing the goniometer, the recorder will indicate level changes in stress as to compressive or tensile stress and magnitudes. Fastress is now in use to monitor products such as heat treated bearings, check carburized parts for tensile stresses (which indicate de-

carburization), and determine the extent of residual stresses generated during surface finishing operations. Residual stress measurements on fatigued and nonfatigue specimens of each type of steel, below and above the endurance limit were taken. Three readings were taken on each bar and the average value computed.

5.2.7. Steel Cleanliness

The cleanliness of each type of steel was examined in accordance with the ASM Standard E45 [43]. Specimens were cut from a test bar of each type of steel and the longitudinal cross-sectional planes were ground and polished. The polished surfaces were examined under a microscope at a 100X magnification and the type of inclusions observed were compared directly against a standard chart to determine the classification according to the JK Rating.

5.3 RESULTS AND DISCUSSION

5.3.1. Fatigue Test Results

Fatigue test results on standard production 8650H, 4340 and 4140 steels, stress shot peened 8650H and 4340, nitrided 4140 and carburized 8620 and 1045 tank track pins are listed in Tables 5-3 through 5-9 and shown in Figures 5-7 through 5-11. The summary of S-N Curves for these above steels is presented in Figure 5-11.

5.3.1.1. Stress Shot Peened 8650H. Stress shot peening of standard production 8650H pins provides the greatest improvement in the fatigue strength of the tank track pins. The endurance limit is raised from 155 ksi [39] for the standard production pin to 198 ksi for the stress shot peened 8650H pin as shown in Figure 5-7 and Table 5-3. Stress shot peening has been reported to improve the fatigue strength of many machine components which are subjected to unidirectional fatigue loads [22]. The major contribution to the increase in the fatigue strength of a stress shot peened part is attributed to the large increase in the compressive residual stress at the surface of the part. The effect of stress shot peening on the residual stress pattern in the pin is illustrated in Figure 5-12.

The high surface compressive stress in the pin is accomplished in the following manner. The pin is first loaded in tension to a tensile stress of 87 ksi before peening. The entire surface of the pin in then shot peened while it is in tension. A thin layer in the surface, about 0.010 inch deep, is plastically deformed by the peening and is placed into compression to -125 ksi or about half the yield strength. When the tensile load is released, all of the elastic strain is removed by elastic recovery except the plastic portion induced by the peening. The total surface residual stress is now

Table 5-3. Fatigue Test Results on Stress Shot Peened 8650H Steel Pins

Maximum Stress (ksi)	Life (Cycles)
252	103,250
228	509,180
203	988,210
200	1,068,230
198	2,000,000*
178	2,000,000*
178	2,000,000**

* did not fail
** specimen rotated 90°

Table 5-4. Fatigue Test Results on Stress Shot Peened 4340 Steel Pins

Maximum Stress (ksi)	Life (Cycles)
203	68,350
173	206,260
171	166,710
168	2,000,000*

* did not fail

Table 5-5. Fatigue Test Results on Induction Hardened and Shot Peened 4340 Pins

Maximum Stress (ksi)	Life (Cycles)
294	27,100
215	63,530
200	103,240
185	128,260
181	121,040
178	130,390
175	2,000,000*
173	169,070
171	111,590
169	2,000,000*
166	87,360

* did not fail

Table 5-6. Fatigue Test Results on Induction Hardened and Shot Peened 4140 Pins

Maximum Stress (ksi)	Life (Cycles)
220	51,850
190	138,440
178	126,940
176	2,000,000*
172	113,440
169	116,450
164	281,070
162	247,690
160	2,000,000*

* did not fail

Table 5-7. Fatigue Test Results on Nitrided and Shot Peened 4140

Maximum Stress (ksi)	Life (Cycles)
205	40,510
190	95,540
176	145,210
166	243,940
163	220,710
160	2,000,000*
153	2,000,000*

* did not fail

Table 5-8. Fatigue Test Results on Carburized 8620 Pins

Maximum Stress (ksi)	Life (Cycles)
197	49,640
182	80,110
176	220,950
174	2,000,000*
171	2.000,000*

* did not fail

Table 5-9. Fatigue Test Results on Carburized 1045 Pins

Maximum Stress (ksi)	Life (Cycles)
172	8,750
144	17,770

* did not fail

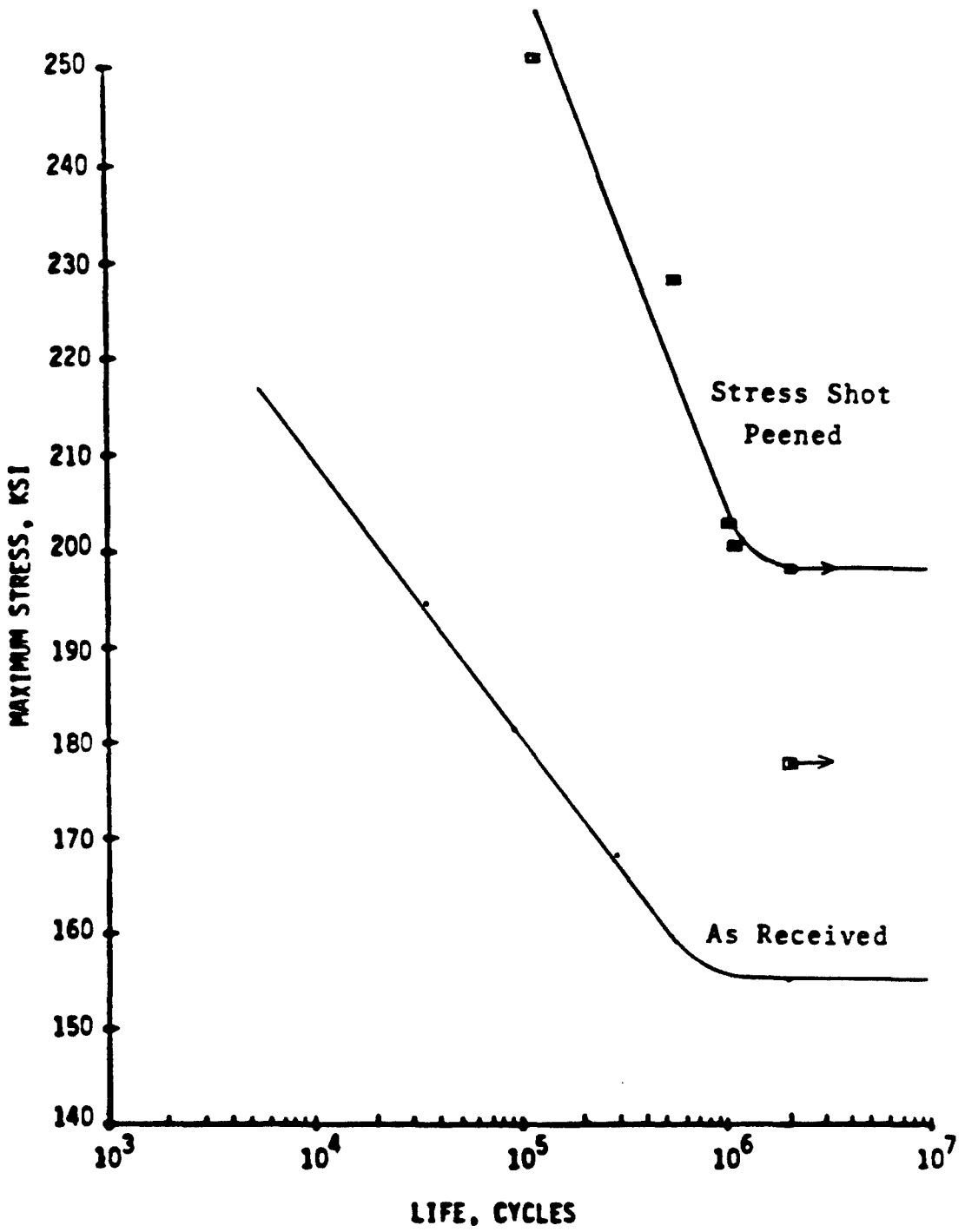

Figure 5-7. S-N Curves for Induction Hardened SAE 8650H Steel Pins.

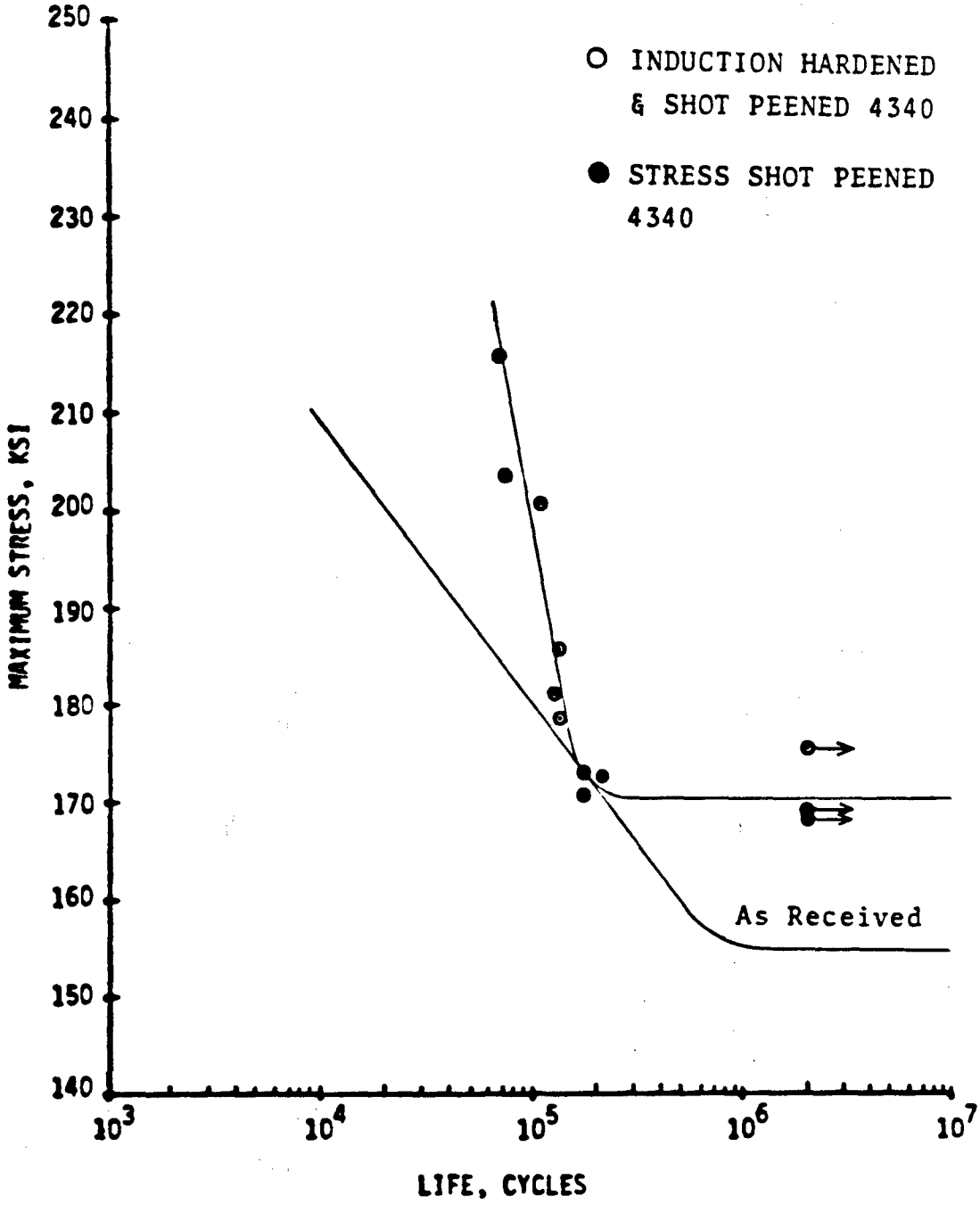

Figure 5-8. S-N Curve for Induction Hardened SAE 4340 Steel Pins.

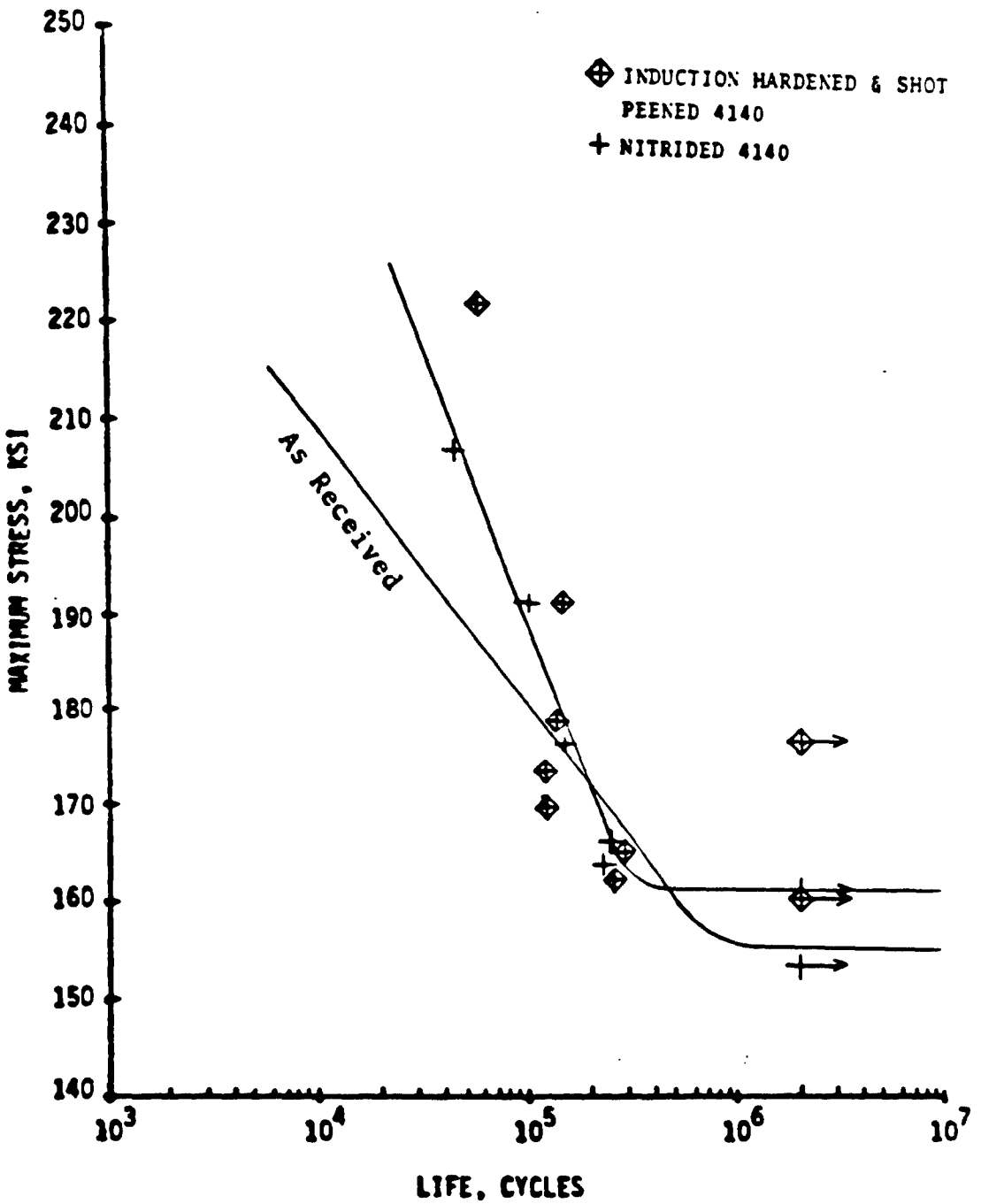

Figure 5-9. S-N Curve for Induction Hardened and Nitrided 4140 Steel Pins.

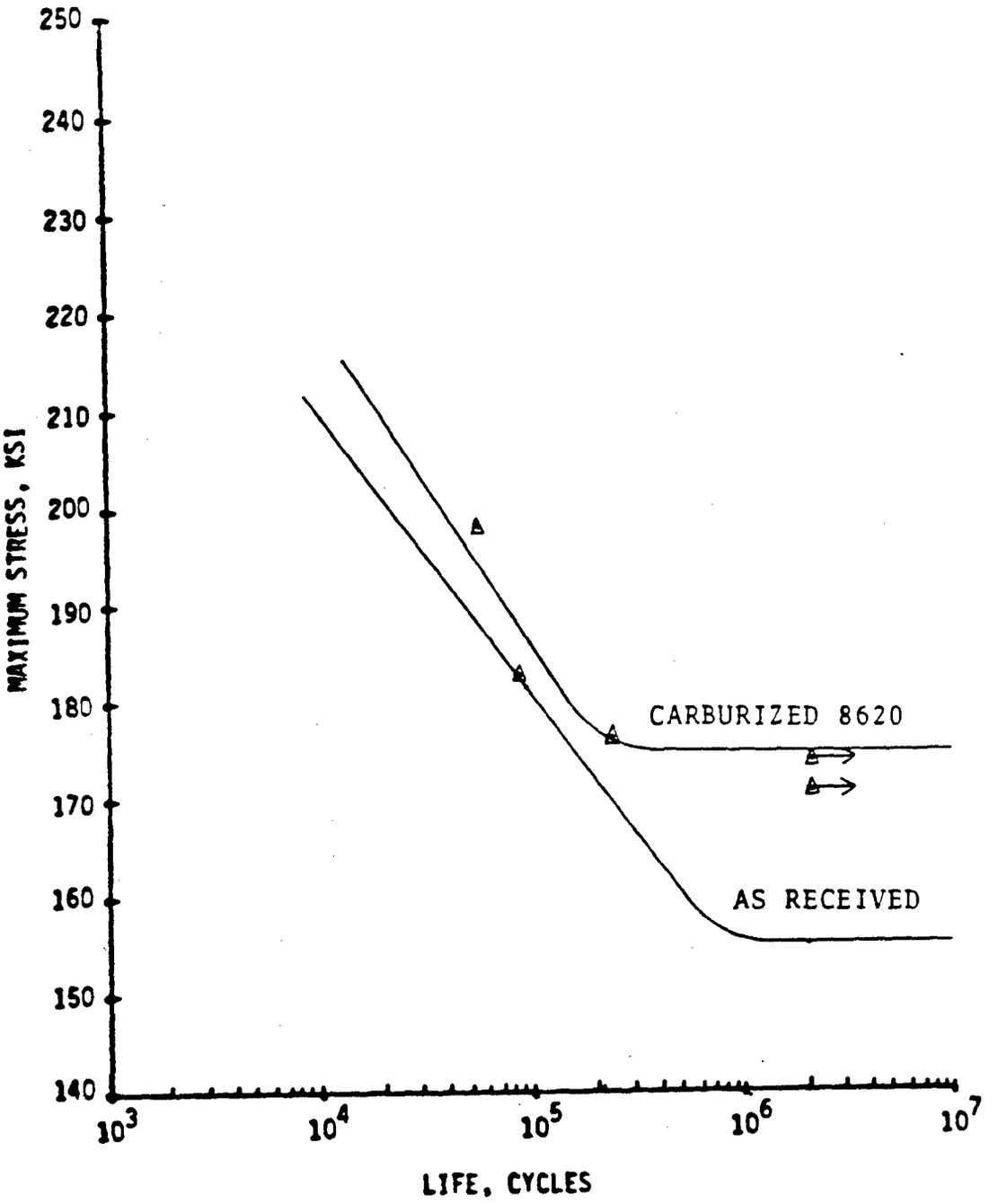

Figure 5-10. S-N Curve for Carburized 8620 Steel Pins.

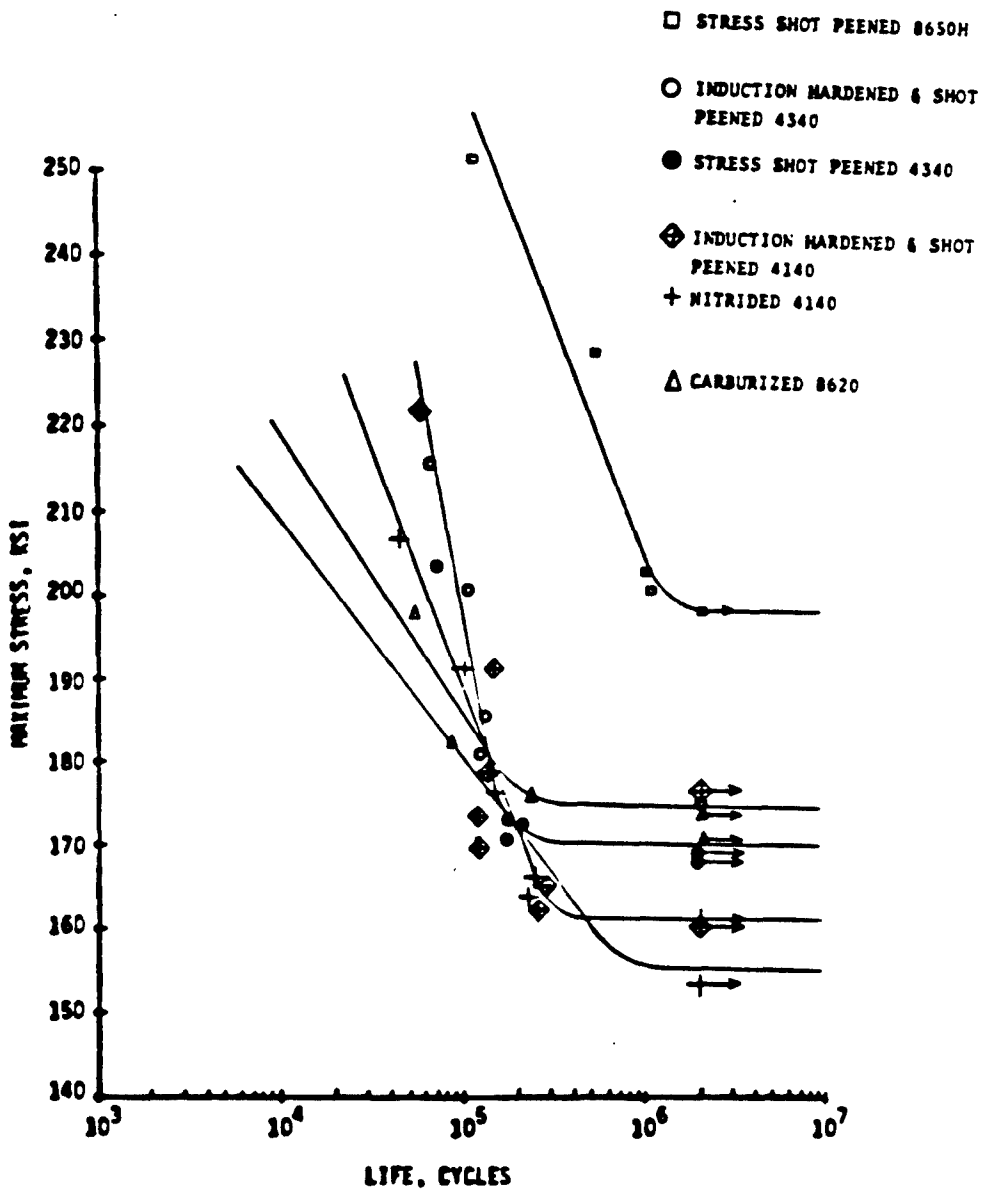

Figure 5-11. S-N Curves for All Tank Track Pins.

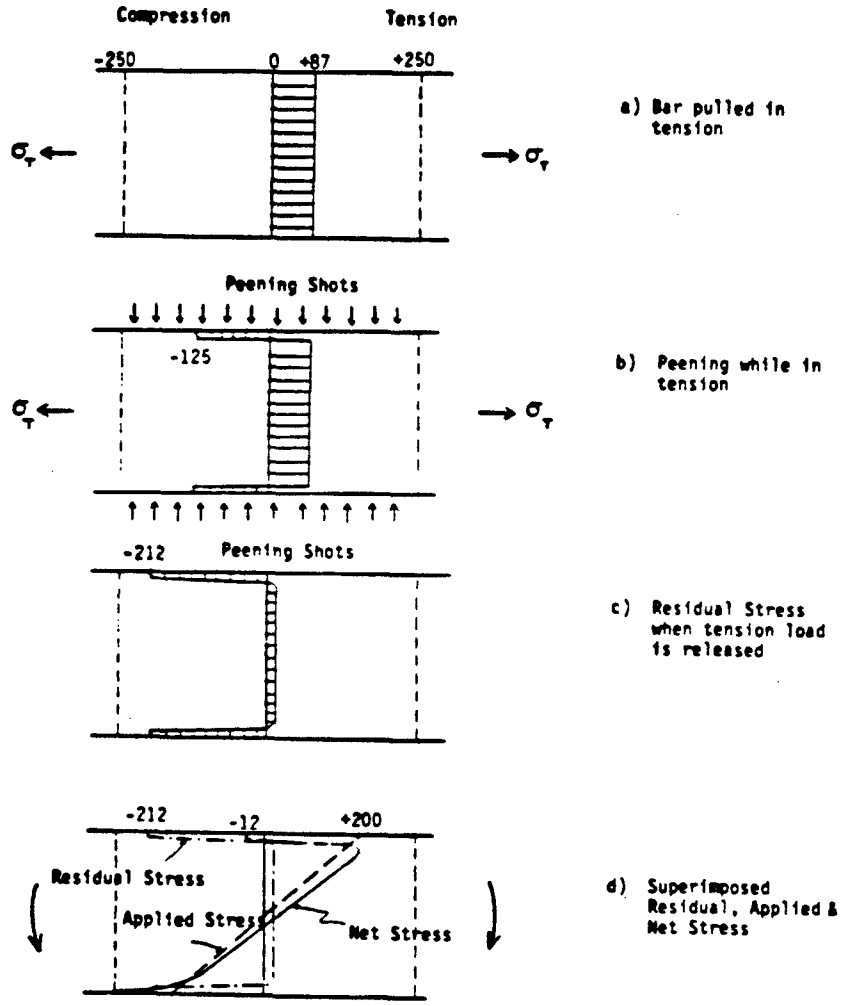

Figure 5-12. Stress Pattern with Stress Shot Peening.

-212 ksi. This is nearly double the -110 ksi surface residual stress measured on the conventionally shot peened regular production 8650H pin. When a maximum bending stress of 200 ksi is applied, the thin layer in the surface, about 0.01 inch deep, still remains in compression to a net stress of -12 ksi. As a result, a fatigue crack cannot start from the outer surface since it is under compression even when subjected to a high bending stress. The last illustration in Figure 5-12 shows the superimposed residual, bending and net stresses on the cross section of the pin. A high tensile stress which predicts subsurface failure. Observations of the fatigue fracture surfaces of the 8650H pins revealed subsurface failure with a crack initiation site at a region just under the case-core interface as shown by the arrow in Figure 5-13. A similar subsurface failure in a carburized differential cross has been reported by Breen and Wene [17]. In contrast, the regular production 8650H pins which were conventionally shot peened, revealed crack origins at the outer surface as shown in Figure 5-14 [39]. The surface residual stress of -110 ksi as measured on this pin is not high enough to strengthen the surface sufficiently to avoid fatigue crack initiation at this site. The net stress on the surface remains tensile and is only reduced to 90 ksi when subjected to a maximum bending stress of 200 ksi as illustrated in Figure 5-15. Since the surface produced from shot peening is rough and has some stress raisers, the presence of tensile stresses favor crack origin at the surface.

5.3.1.2. Stress Shot Peened 4340. The fatigue test results on stress shot peened 4340 pins are listed in Table 5-4 and the S-N curve shown in Figure 5-8. Although these pins might be expected to perform somewhat better than the stress shot peened 8650H pins because of its superior hardenability, the results did not indicate so. The endurance limit of stress shot peened 4340 is 170 ksi compared to 198 ksi for the stress shot peened 8650H pins. The fatigue fracture surfaces of the 4340 pins did not reveal subsurface failure as in the case of 8650H pins but instead showed fatigue cracks that originated from the inner surface as indicated by the arrow in Figure 5-16. The compressive residual stress at the outer surface have the same magnitude as that of 8650H which is -212 ksi. When a maximum bending stress of 200 ksi is applied, this high compressive stress keeps the surface in compression with a net stress of -12 ksi. This sufficiently strengthens the outer surface since the stress does not become high enough for a fatigue crack to develop. The 4340 pins have a 0.6 inch bore hole diameter which is 0.1 inch larger than that of as received 8650H pins. Plots of stress and strength gradients across the cross section of the two pins (Figures 5-17 and 5-18), show insufficient strength gradient in the core to resist the applied stress gradient. The tensile stress at the inner surface of 4340 pin is 16 ksi larger than that of 8650H when subjected to equal bending stress of 200 ksi (see also Tables 5-10 and 5-11). Apparently the larger bore diameter has a greater effect than anticipated in weakening the inner surface, probably through the increased stress concentration and the higher tensile stress. Accordingly cracks originate at the inner surface

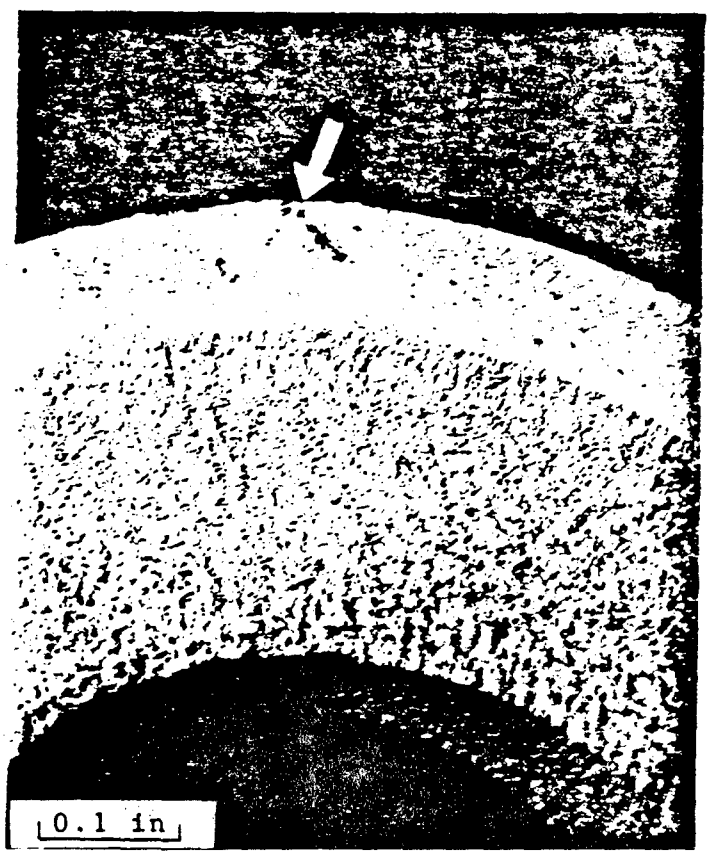

Figure 5-13. **Fracture Surface of an As Received Pin Showing a Fatigue Crack Origin at the Surface.**

Figure 5-14. Fracture Surface of a Stress Shot Peened 8650H Pin. Arrow Shows a Subsurface Fatigue Crack Origin.

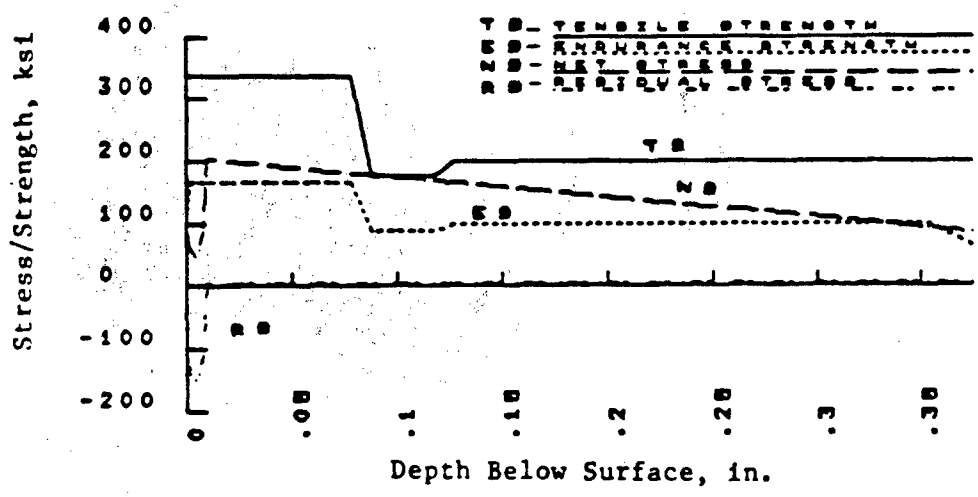

Figure 5-15. Stress and Strength Distribution in As Received 8650H Pin.

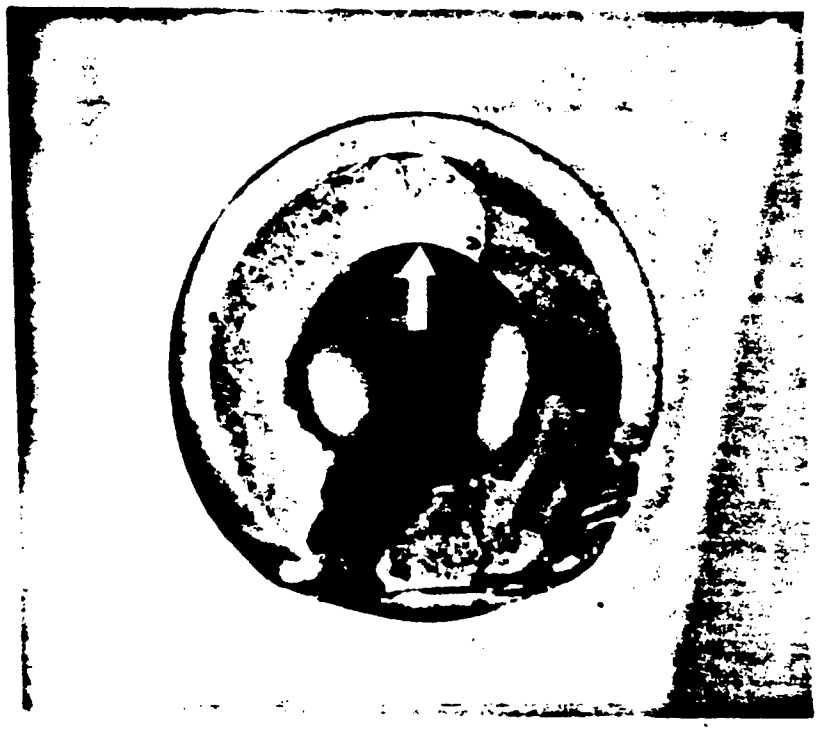

Figure 5-16. Fracture Surface of a Stress Shot Peened 4340 Pin. Arrow Shows a Fatigue Crack Origin at the Inner Surface (σ_{max}=203 ksi, N_f=68,350 cycles). 2X

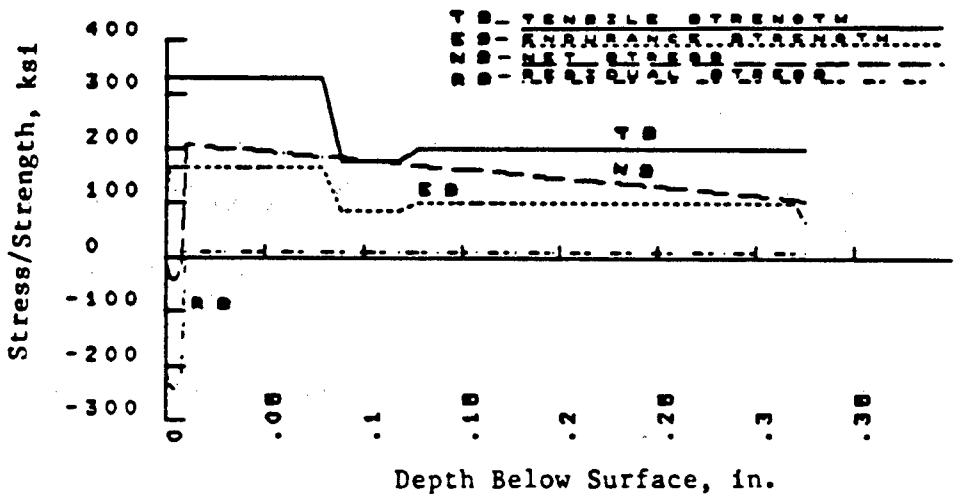

Figure 5-17. Stress and Strength Distribution in a Stress Shot Peened 4340 Pin. Applied σ_{max}=200 ksi.

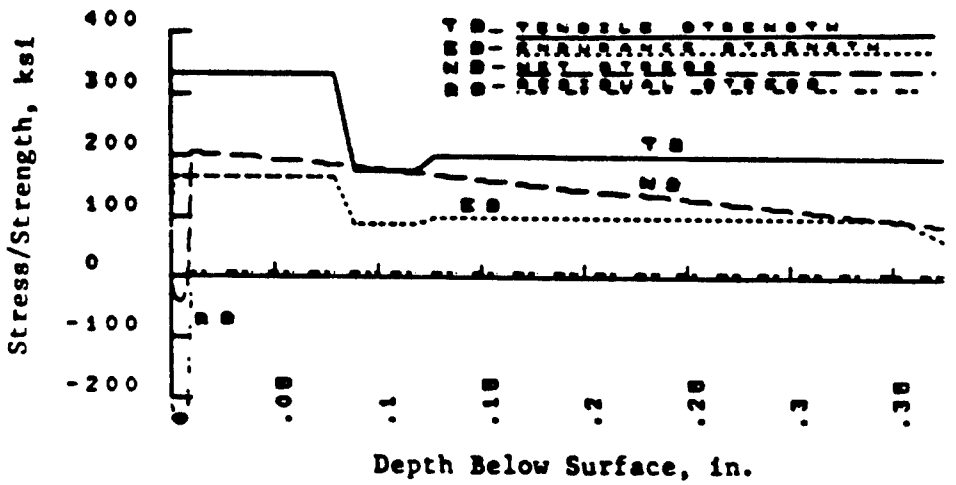

Figure 5-18. Stress and Strength Distribution in a Stress Shot Peened 8650H Pin. Applied σ_{max}=200 ksi.

Table 5-10. Stress and Strength Distribution in Stress Shot Peened 4340 Pin

DEPTH (in)	TENSILE STR (ksi)	SURFACE FACTOR	ENDURANCE STR (ksi)	RESIDUAL STR (ksi)	BENDING STR (ksi)	NET STR (ksi)
0	330	.66	108.9	-212	200	-12
.19685E-02	330	1	165	-234.5	199.37	-35.1299
.393701E-02	330	1	165	-242	198.74	-43.2598
.590551E-02	330	1	165	-234.5	198.11	-36.3898
.787402E-02	330	1	165	-212	197.48	-14.5197
.984252E-02	330	1	165	9.12072	196.85	205.971
.019685	330	1	165	9.12072	193.701	202.822
.295276E-01	330	1	165	9.12072	190.551	199.672
.393701E-01	330	1	165	9.12072	187.402	196.522
.492126E-01	330	1	165	9.12072	184.252	193.373
.590551E-01	330	1	165	9.12072	181.102	190.223
.688976E-01	330	1	165	9.12072	177.953	187.073
.787402E-01	330	1	165	9.12072	174.803	183.924
.885827E-01	175	1	87.5	9.12072	171.654	180.774
.984252E-01	175	1	87.5	9.12072	168.504	177.625
.108268	175	1	87.5	9.12072	165.354	174.475
.11811	175	1	87.5	9.12072	162.205	171.325
.127953	200	1	100	9.12072	159.055	168.176
.137795	200	1	100	9.12072	155.906	165.026
.147638	200	1	100	9.12072	152.756	161.877
.15748	200	1	100	9.12072	149.606	158.727
.167323	200	1	100	9.12072	146.457	155.577
.177165	200	1	100	9.12072	143.307	152.428
.187008	200	1	100	9.12072	140.157	149.278
.19685	200	1	100	9.12072	137.008	146.129
.212598	200	1	100	9.12072	131.969	141.089
.248031	200	1	100	9.12072	120.63	129.751
.283465	200	1	100	9.12072	109.291	118.412
.318898	200	1	100	9.12072	97.9528	107.073
.325	200	.66	66	9.12072	96	105.121

Table 5-11. Stress and Strength Distribution in Stress Shot Peened 8650H Pin

DEPTH (in)	TENSILE STR (ksi)	SURFACE FACTOR	ENDURANCE STR (ksi)	RESIDUAL STR (ksi)	BENDING STR (ksi)	NET STR (ksi)
0	330	.66	108.9	-212	200	-12
.19685E-02	330	1	165	-234.5	199.37	-35.1299
.393701E-02	330	1	165	-242	198.74	-43.2598
.590551E-02	330	1	165	-234.5	198.11	-36.3898
.787402E-02	330	1	165	-212	197.48	-14.5197
.984252E-02	330	1	165	9.12072	196.85	205.971
.019685	330	1	165	9.12072	193.701	202.822
.295276E-01	330	1	165	9.12072	190.551	199.672
.393701E-01	330	1	165	9.12072	187.402	196.522
.492126E-01	330	1	165	9.12072	184.252	193.373
.590551E-01	330	1	165	9.12072	181.102	190.223
.688976E-01	330	1	165	9.12072	177.953	187.073
.787402E-01	330	1	165	9.12072	174.803	183.924
.885827E-01	175	1	87.5	9.12072	171.654	180.774
.984252E-01	175	1	87.5	9.12072	168.504	177.625
.108268	175	1	87.5	9.12072	165.354	174.475
.11811	175	1	87.5	9.12072	162.205	171.325
.127953	200	1	100	9.12072	159.055	168.176
.137795	200	1	100	9.12072	155.906	165.026
.147638	200	1	100	9.12072	152.756	161.877
.15748	200	1	100	9.12072	149.606	158.727
.167323	200	1	100	9.12072	146.457	155.577
.177165	200	1	100	9.12072	143.307	152.428
.187008	200	1	100	9.12072	140.157	149.278
.19685	200	1	100	9.12072	137.008	146.129
.23622	200	1	100	9.12072	124.409	133.53
.275591	200	1	100	9.12072	111.811	120.932
.314961	200	1	100	9.12072	99.2126	108.333
.354331	200	1	100	9.12072	86.6142	95.7349
.375	200	.66	66	9.12072	80	89.1207

instead of at the case-core boundary. The rough surface finish (125 micro-inch) of the inner surface, which is of drill finish quality, could also contribute to this cracking at the bore surface.

5.3.1.3. Induction Hardened and Shot Peened 4340. Fatigue test results on induction hardened and shot peened 4340 pins are listed in Table 5-5 and the S-N curve shown in Figure 5-8. The results indicate no significant difference between the fatigue limit of the the induction hardened pins and the stress shot peened 4340. For this reason, only a single curve is drawn for the two type of pins, both with a fatigue limit of 170 ksi. However, the fracture surfaces of induction hardened pins exhibited two different type of crack origins which indicate that they experienced different modes of fatigue failure. These two types of crack origins are indicated by the arrows in Figures 5-19 and 5-20. At maximum bending stress level of about 180 ksi and above, crack origins were observed to be at the outer surface. At bending stresses below 180 ksi, crack origins were found to be at the inner surface of the pins. The stress-strength gradient analysis for maximum and minimum applied loads are illustrated in Figures 5-21 and 5-22 and Tables 5-12 and 5-13. These figures indicate that subsurface failure should occur at the case-core interface of the induction hardened pin. Nevertheless, no such failure was observed in any of the failed specimens. The compressive residual stress at the surface is not high enough to keep the surface in a compressive region. At high bending stresses above 180 ksi, the tensile stress at the surface is high enough to produce significant tensile stresses and to cause crack to originate at the outer surface. However, at low bending stresses, below 180 ksi, the tensile stresses at the inner surface that is not shot peened becomes high enough to cause cracking to start at this surface. Figures 5-23 and 5-24 show fatigue cracks arrested in the pin before total fracture occurs. These cracks were initiated at the innner surface and have travelled to the outer surface. AB in Figure 5-24 represents the fatigue crack propagation zone while BD is the instantaneous failure region when the remaining cross-sectional area could no longer sustain the applied load. CD is the instantaneous crack portion through the induction hardened layer.

5.3.1.4. Induction Hardened and Shot Peened 4140. The induction hardened and shot peened 4140 pins has a fatigue limit of 160 ksi as shown in Figure 5-9. The detailed fatigue test results are listed in Table 5-6. The short life portion of the S-N curve has a steeper gradient and the knee of the curve occurs at a lower number of cycles than that of the as received 8650H pin. Examination of the fatigue fracture surfaces of the 4140 pins indicated a similar failure mode to that of induction hardened and shot peened 4340 pins. Fatigue crack origins occurred at the outer surface of the pin at high bending stresses, above 180 ksi. At low bending stresses, below 180 ksi, fatigue crack origins at the inner surface of the pin were observed. The numerous shear lips in the core indicate the higher ductility of these pins compared to the as received ones.

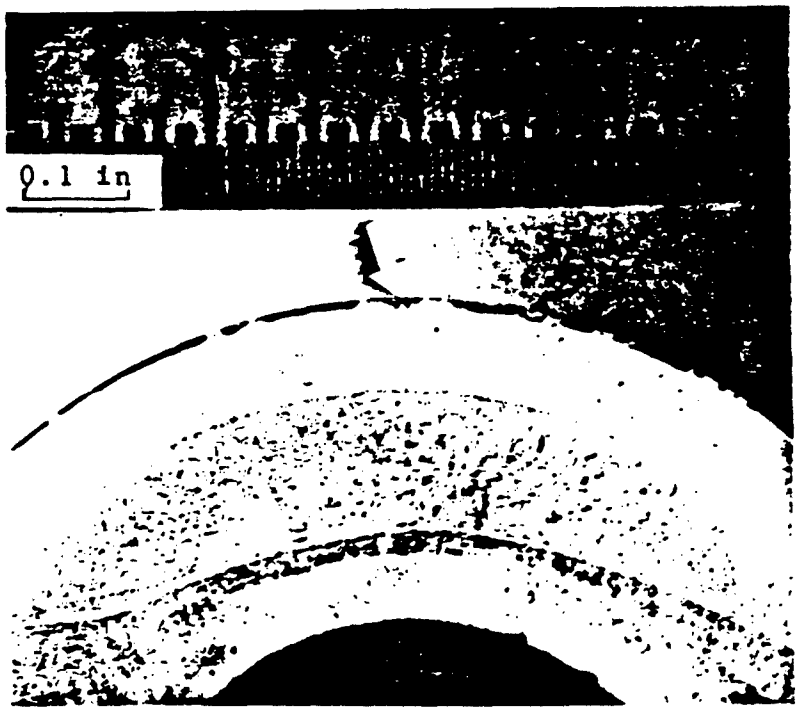

Figure 5-19. **Fracture Surface of an Induction Hardened 4340 Pin with Crack Origin at the Outer Surface.**

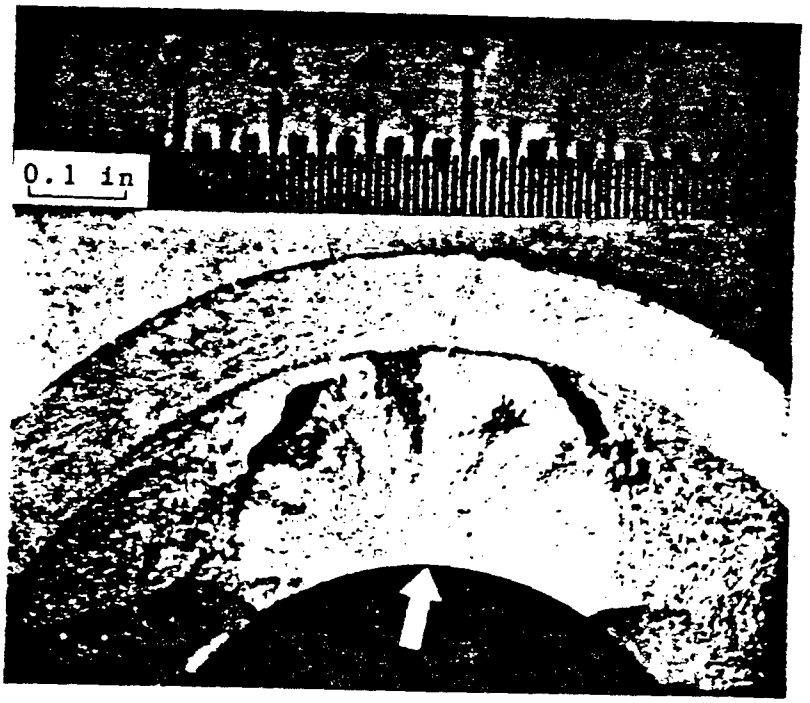

Figure 5-20. Fracture Surface of an Induction Hardened 4340 Pin with Crack Origin at the Inner Surface (σ_{max} = 181 ksi, N_f=121,040 cycles).

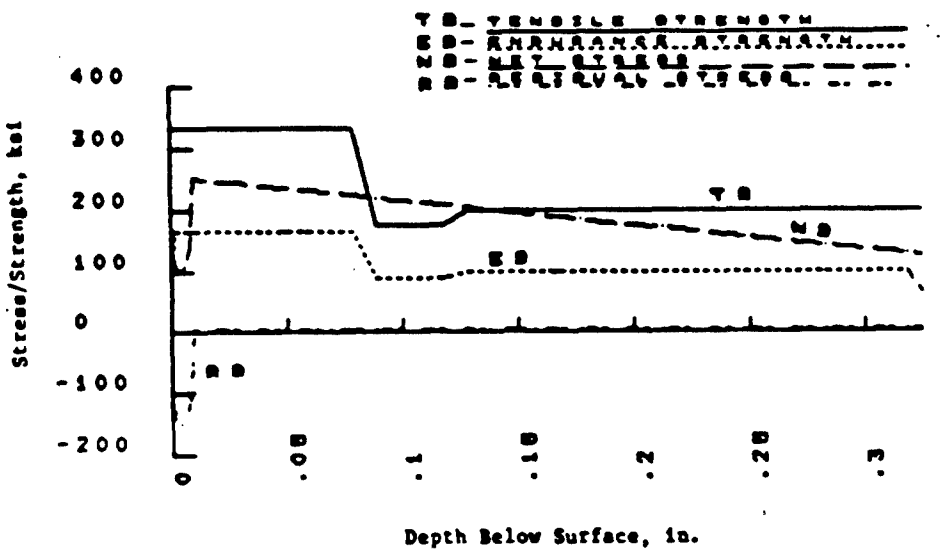

Figure 5-21. Stress and Strength Distribution in an Induction Hardened 4340 Pin with an Applied Bending σ_{max}=250 ksi.

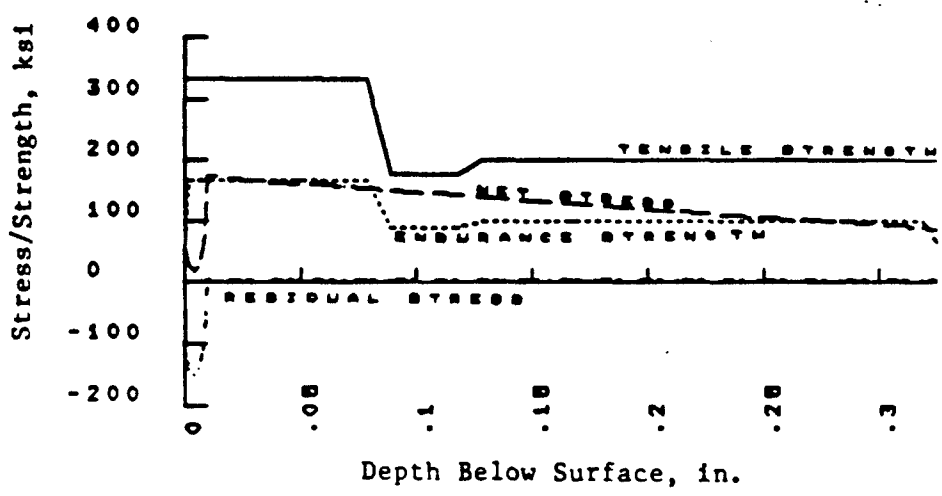

Figure 5-22. Stress and Strength Distribution in an Induction Hardened 4340 Pin with an Applied Bending σ_{max}=168 ksi.

Table 5-12. Stress and Strength Distribution in Induction Hardened 4340 Pin with Bending σ_{max}=250 ksi

DEPTH (in)	TENSILE STR (ksi)	SURFACE FACTOR	ENDURANCE STR (ksi)	RESIDUAL STR (ksi)	BENDING STR (ksi)	NET STR (ksi)
0	330	.66	108.9	-110	250	140
.19685E-02	330	1	165	-140	249.213	109.213
.393701E-02	330	1	165	-150	248.425	98.4252
.590551E-02	330	1	165	-140	247.638	107.638
.787402E-02	330	1	165	-110	246.85	136.85
.984252E-02	330	1	165	4.73245	246.063	250.795
.019685	330	1	165	4.73245	242.126	246.858
.295276E-01	330	1	165	4.73245	238.189	242.921
.393701E-01	330	1	165	4.73245	234.252	238.984
.492126E-01	330	1	165	4.73245	230.315	235.047
.590551E-01	330	1	165	4.73245	226.378	231.11
.688976E-01	330	1	165	4.73245	222.441	227.173
.787402E-01	330	1	165	4.73245	218.504	223.236
.885827E-01	175	1	87.5	4.73245	214.567	219.299
.984252E-01	175	1	87.5	4.73245	210.63	215.362
.108268	175	1	87.5	4.73245	206.693	211.425
.11811	175	1	87.5	4.73245	202.756	207.488
.127953	200	1	100	4.73245	198.819	203.551
.137795	200	1	100	4.73245	194.882	199.614
.147638	200	1	100	4.73245	190.945	195.677
.15748	200	1	100	4.73245	187.008	191.74
.167323	200	1	100	4.73245	183.071	187.803
.177165	200	1	100	4.73245	179.134	183.866
.187008	200	1	100	4.73245	175.197	179.929
.19685	200	1	100	4.73245	171.26	175.992
.212598	200	1	100	4.73245	164.961	169.693
.248031	200	1	100	4.73245	150.787	155.52
.283465	200	1	100	4.73245	136.614	141.347
.318898	200	1	100	4.73245	122.441	127.173
.325	200	.66	66	4.73245	120	124.732

Table 5-13. Stress and Strength Distribution in Induction Hardened 4340 Pin with Bending σ_{max}=168 ksi

DEPTH (in)	TENSILE STR (ksi)	SURFACE FACTOR	ENDURANCE STR (ksi)	RESIDUAL STR (ksi)	BENDING STR (ksi)	NET STR (ksi)
0	330	.66	108.9	-110	168	58
.19685E-02	330	1	165	-140	167.471	27.4709
.393701E-02	330	1	165	-150	166.942	16.9417
.590551E-02	330	1	165	-140	166.413	26.4126
.787402E-02	330	1	165	-110	165.883	55.8835
.984252E-02	330	1	165	4.73245	165.354	170.087
.019685	330	1	165	4.73245	162.709	167.441
.295276E-01	330	1	165	4.73245	160.063	164.795
.393701E-01	330	1	165	4.73245	157.417	162.15
.492126E-01	330	1	165	4.73245	154.772	159.504
.590551E-01	330	1	165	4.73245	152.126	156.858
.688976E-01	330	1	165	4.73245	149.48	154.213
.787402E-01	330	1	165	4.73245	146.835	151.567
.885827E-01	175	1	87.5	4.73245	144.189	148.921
.984252E-01	175	1	87.5	4.73245	141.543	146.276
.108268	175	1	87.5	4.73245	138.898	143.63
.11811	175	1	87.5	4.73245	136.252	140.984
.127953	200	1	100	4.73245	133.606	138.339
.137795	200	1	100	4.73245	130.961	135.693
.147638	200	1	100	4.73245	128.315	133.047
.15748	200	1	100	4.73245	125.669	130.402
.167323	200	1	100	4.73245	123.024	127.756
.177165	200	1	100	4.73245	120.378	125.11
.187008	200	1	100	4.73245	117.732	122.465
.19685	200	1	100	4.73245	115.087	119.819
.212598	200	1	100	4.73245	110.854	115.586
.248031	200	1	100	4.73245	101.329	106.062
.283465	200	1	100	4.73245	91.8047	96.5372
.318898	200	1	100	4.73245	82.2803	87.0128
.325	200	.66	66	4.73245	80.64	85.3725

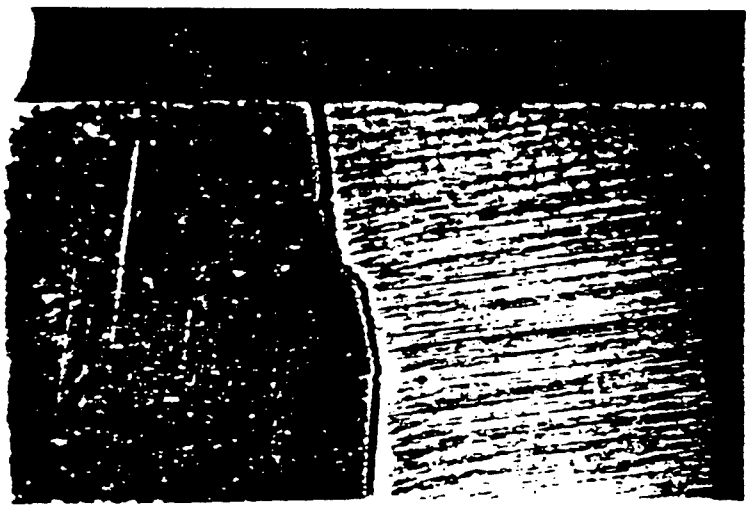

Figure 5-23. A Fatigue Crack that started from the Inner Surface of an Induction Hardened 4340 Pin (σ_{max}=166 ksi, N_f=87,360 cycles), 6.5X

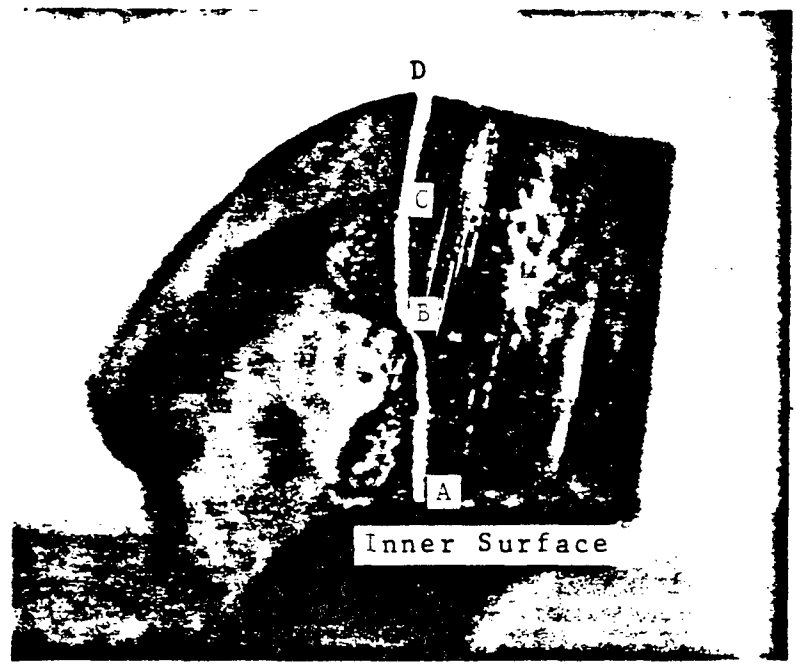

Figure 5-24. A Fatigue Crack Profile in an Induction Hardened 4340 Pin Showing the Various Fatigue Failure Stages (σ_{max}=171 ksi, N_f=111,590 cycles), 6.5X

5.3.1.5. Nitrided and Shot Peened 4140. Fatigue test results for nitrided 4140 pins are listed in Table 5-7. and the S-N curve is shown in Figure 5-9. The results indicate no significant difference from those of induction hardened 4140. Both type of pins have the same fatigue limit of 160 ksi. No significant improvement in the fatigue strength is obtained through this processing technique. The hard nitrided case of the nitrided pin has a relatively low strength just a small distance under the case. Even the case occasionally shows soft areas. Macro and microhardness tests indicated a surface hardness of only 47 Rockwell C at some spots and a core hardness of 35 Rockwell C. This is rather low when compared to the desired hardness of 60-62 Rockwell C at the surface and 40-45 Rockwell C in the core in the other pins. Examination of the surface microstructure revealed a white layer of about 100 to 200 microinch thick at the outer surface as shown in Figure 5-25. The inner surface has a thicker white layer of about 200 to 300 microinch. Within the nitride layer a reasonable hardness of 54-56 Rockwell C was measured. Figure 5-26 shows a fatigue fracture surface of a nitrided 4140 pin indicating clearly the ductile nature of the core. The arrow indicates crack origin at the outer surface. Similar crack origins were observed in all failed specimens.

5.3.1.6. Carburized 8620. The fatigue limit of carburized 8620 pins was determined to be 175 ksi. The detailed fatigue test results are listed in Table 5-8 and the S-N curve is shown in Figure 5-10. The short life portion of the S-N curve has approximately the same gradient as the as received pins. The knee of the curve occurs at a shorter number of cycles than that of the as received pins. The fatigue fracture surfaces of the carburized pins exhibited almost a flat surface with a woody texture indicating a completely brittle fracture, as shown in Figure 5-27. No fatigue striation marks were observed which indicate that most of its fatigue life is spent in the crack initiation stage. Once the crack is developed, it grows rapidly and leads to final fracture.

5.3.1.7. Carburized 1045. These pins exhibit the lowest fatigue strength of all the pins tested. The fatigue test results in Table 5-9 show a life of only 8,750 cycles when fatigued at a maximum stress of 172 ksi and 17,770 cycles at 144 ksi. In contrast, the carburized 8620 pin did not fail when fatigued at 171 ksi since the stress is below their endurance limit. The fracture surfaces of the pins exhibit similar features as that of 8620 pins, indicating a total brittle fracture as shown in Figure 5-28. It is noted that the surface of the pins were not shot peened and therefore has a very low surface compressive residual stress which was measured to be -30 ksi. Since these pins exhibit inferior fatigue strength, no further fatigue tests were conducted. The use of this steel with its specialized heat treatment was designed to produce a very high residual stress at the surface (40). Obviously, the processing in this investigation was unsuccessful in attaining this residual stress.

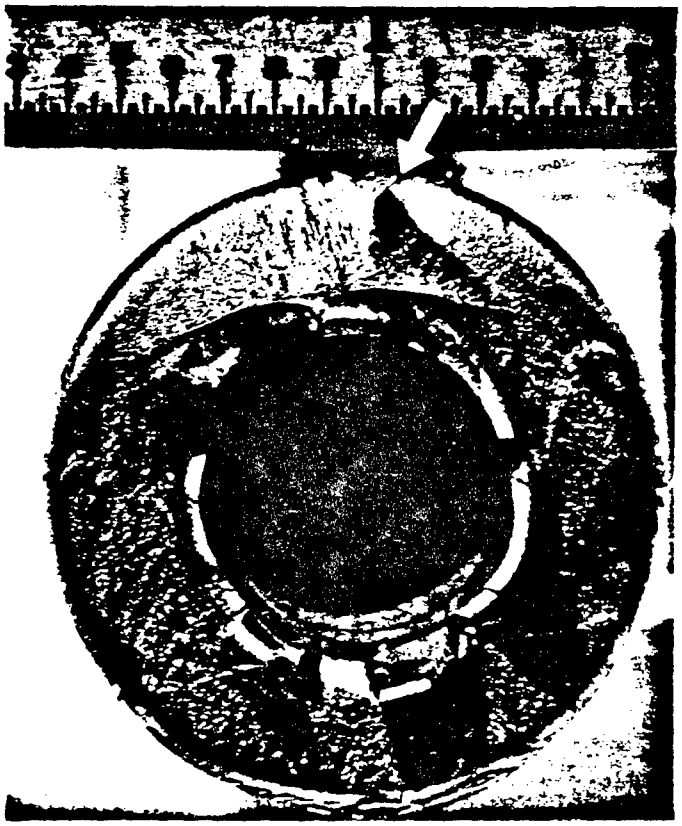

Figure 5-25. Fracture Surface of a Nitrided 4140 Pin showing Crack Origin at the Outer Surface (σ_{max}=205 ksi, N_f=27,100 cycles).

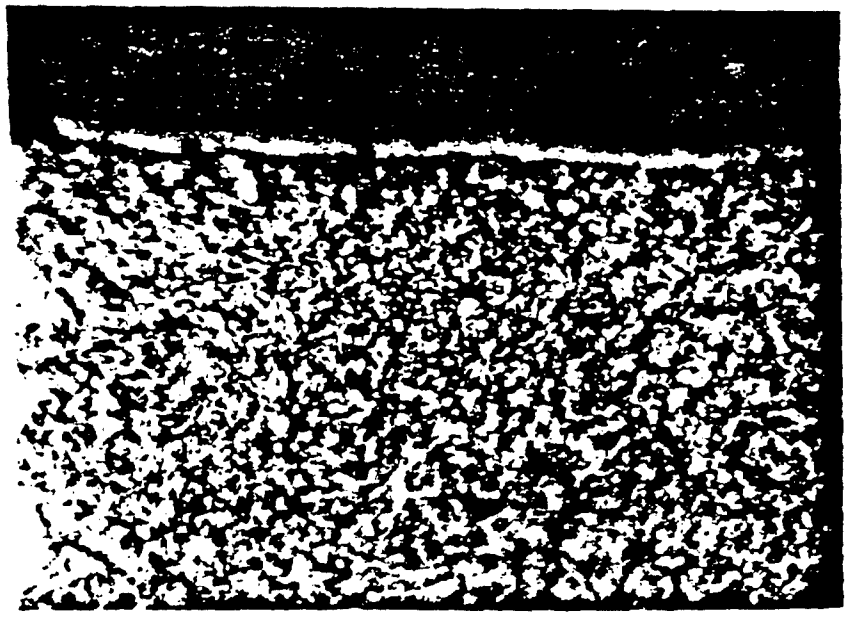

Figure 5-26. Surface Microstructure of a Nitrided 4140 Pin Showing a White Layer of 0.0001 to 0.0002 inch Thick. 600X

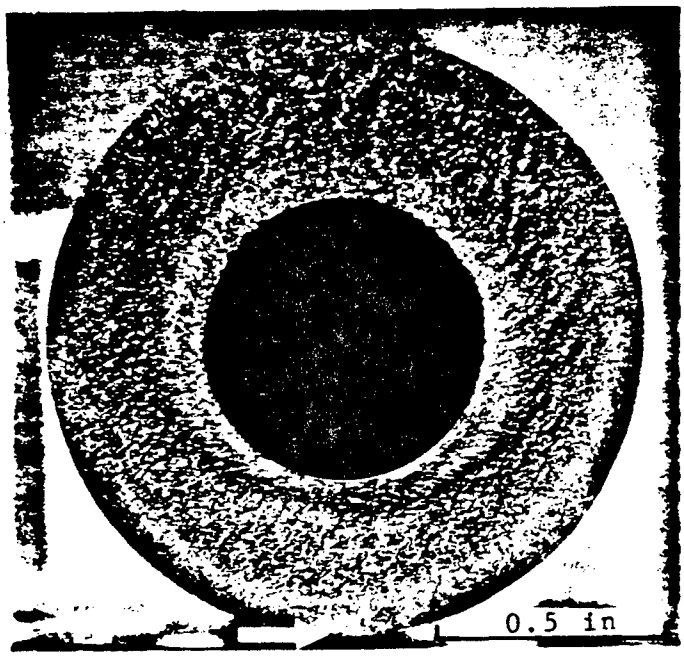

Figure 5-27. Fracture Surface of a Carburized 8620 Pin (σ_{max}=197 ksi, N_f=49,640 cycles).

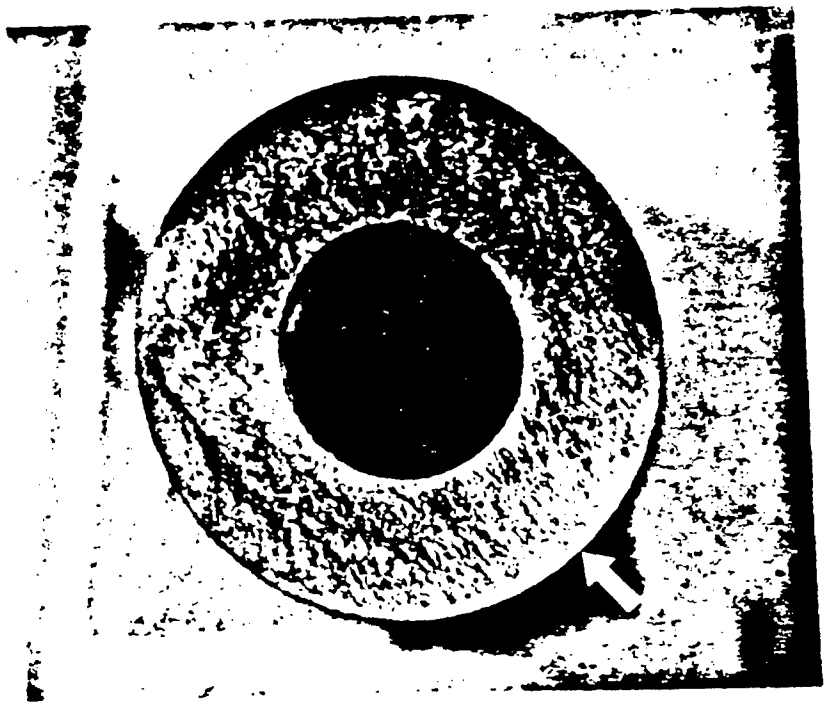

Figure 5-28. Fracture Surface of a Carburized 1045 Pin (σ_{max}=172 ksi, N_f=49,640 cycles). 2X

5.3.2. Microhardness Test Results

5.3.2.1. Stress Shot Peened 8650H. The microhardness pattern in these pins is shown in Figure 5-29. Within the induction hardened layer, the hardness ranges from Rc 59.5 near the outer surface to Rc 57 near the case-core boundary. It drops sharply to Rc 35 in the case-core region which had been slightly tempered during the induction hardening process and then rises to about Rc 43 in the core. The induction hardened layer is about 0.09 inch thick. This hardness pattern fits well with the required hardness specified in drawing number 11645132 as indicated in Figure 2-1.

5.3.2.2. Stress Shot Peened 4340. These pins which have been similarly processed as that of 8650H, exhibit similar hardness patterns ranging from Rc 59 in the induction hardened layer to Rc 35 in the case-core boundary and Rc 41 in the core as illustrated in Figure 5-30. The induction hardened layer is about 0.095 inch thick.

5.3.2.3. Induction Hardened and Shot Peened 4340. The hardness pattern of these pins, as shown in Figure 5-31, are very similar to the stress shot peened 4340 since they have been heat treated in a similar manner.

5.3.2.4. Induction Hardened and Shot Peened 4140. Figure 5-32 shows the hardness pattern in these pins. The hardness in the induction hardened layer is about Rc 58, the case-core region Rc 34.5 and the core Rc 41. The induction hardened layer is about 0.09 inch thick.

5.3.2.5. Nitrided 4140. These pins have a surprisingly low spotty hardness of Rc 46 at some surface locations, as shown in Figure 5-33. In the nitrided layer, the hardness is sufficiently high at Rc 56. Within a thick-ness of about 0.03 inch from either the outer or inner surface of the pin, the hardness drops sharply and levels to about Rc 34 in the core.

5.3.2.6. Carburized 8620. Figure 5-34 shows the hardness profile of carburized 8620 pins. As expected, the surface has a very high hardness of Rockwell C 62. The hardness decreases at a less steeper gradient than the nitrided one to a hardness of about Rc 46 in the mid core position. It then rises at a similar gradient to a hardness of Rc 63 near the inner surface.

5.3.2.7. Carburized 1045. This pin has similar hardness profile to that of 8620. Figure 5-35 shows a hardness ranging from Rc 62 at the outer surface to a Rc 39 in the mid core position and Rc 62 at the inner surface.

5.3.3. Inclusion Content of Test Steels

Examination of the inclusion content in each type of steel showed that they are fairly clean and all can be categorized under the D2 classification of

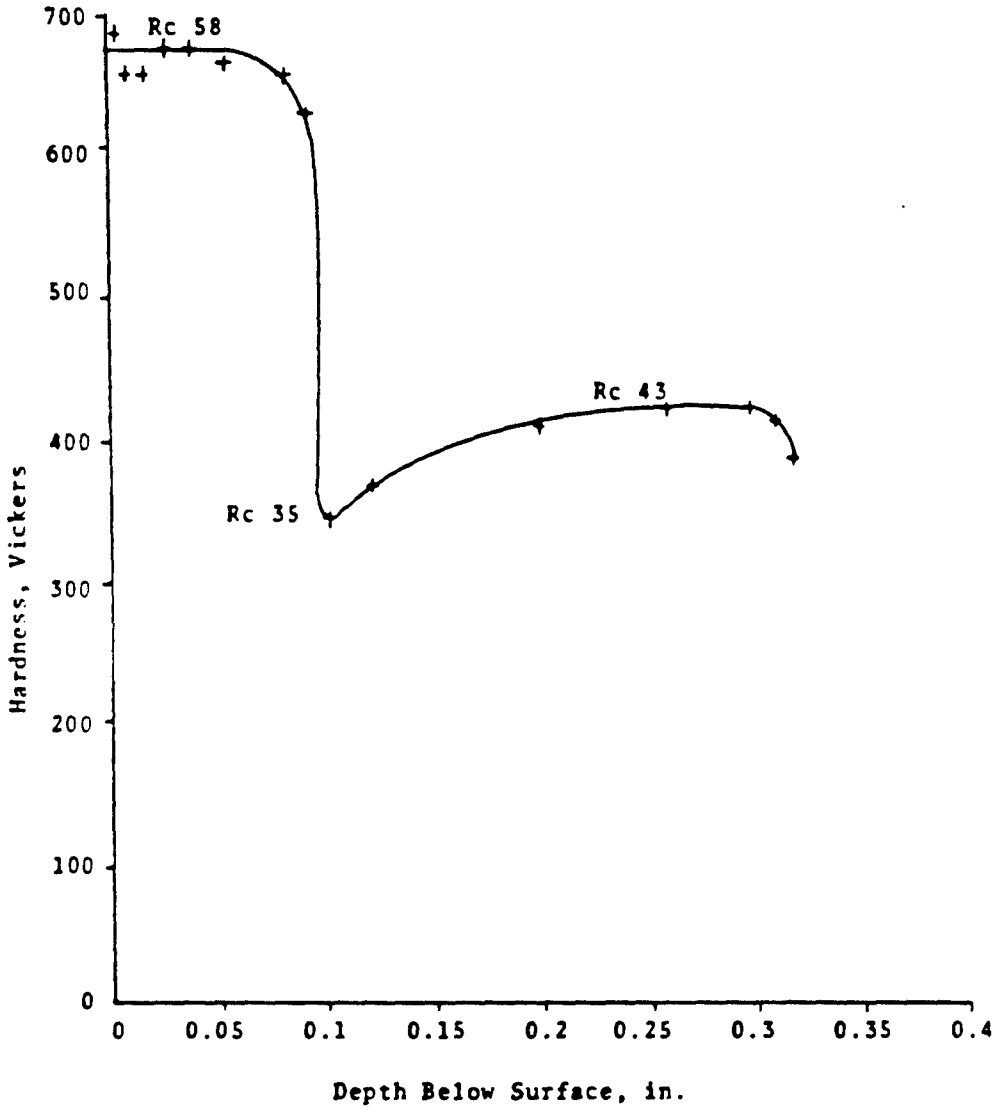

Figure 5-29. Hardness Profile of Stress Shot Peened 8650H Pin.

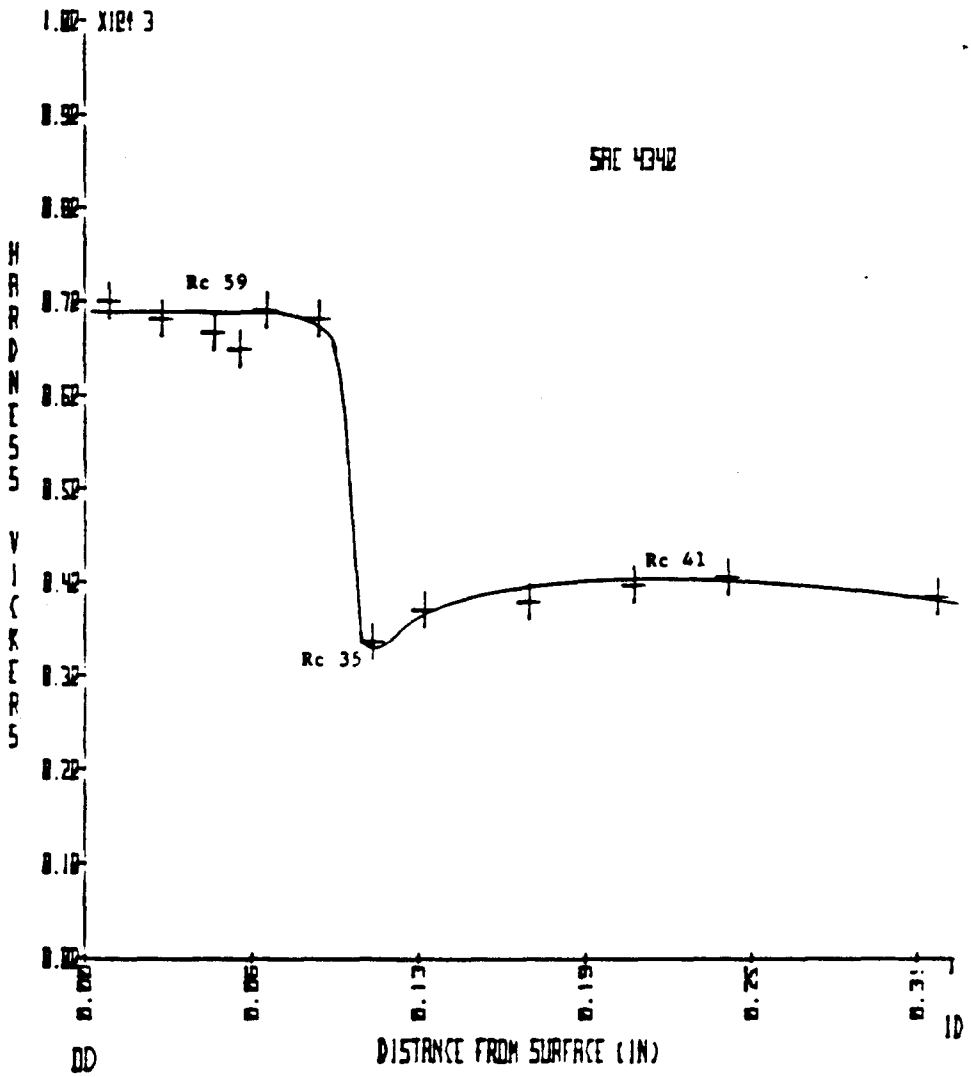

Figure 5-30. Hardness Profile of Stress Shot Peened 4340 Pin.

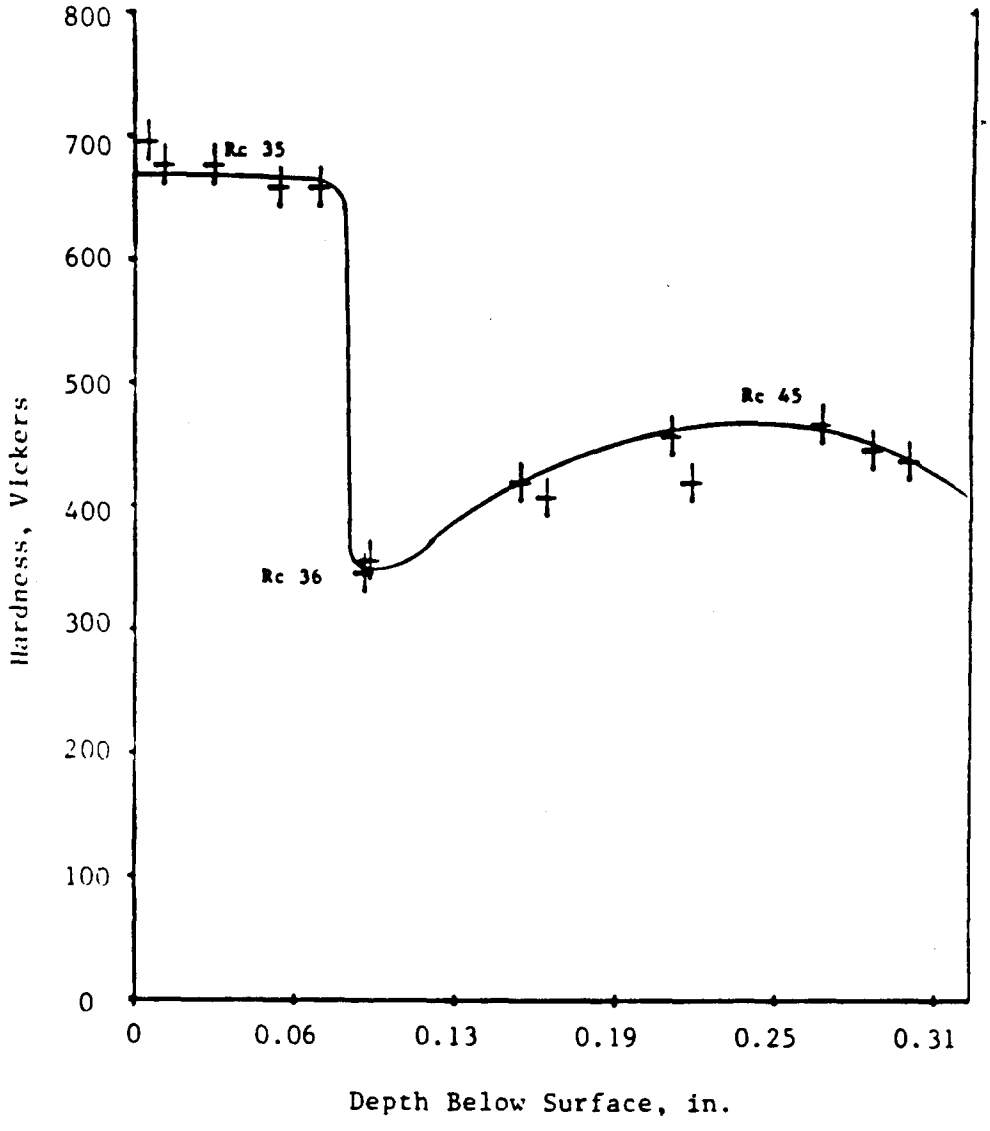

Figure 5-31. Hardness Profile of Regular Shot Peened 4340 Pin.

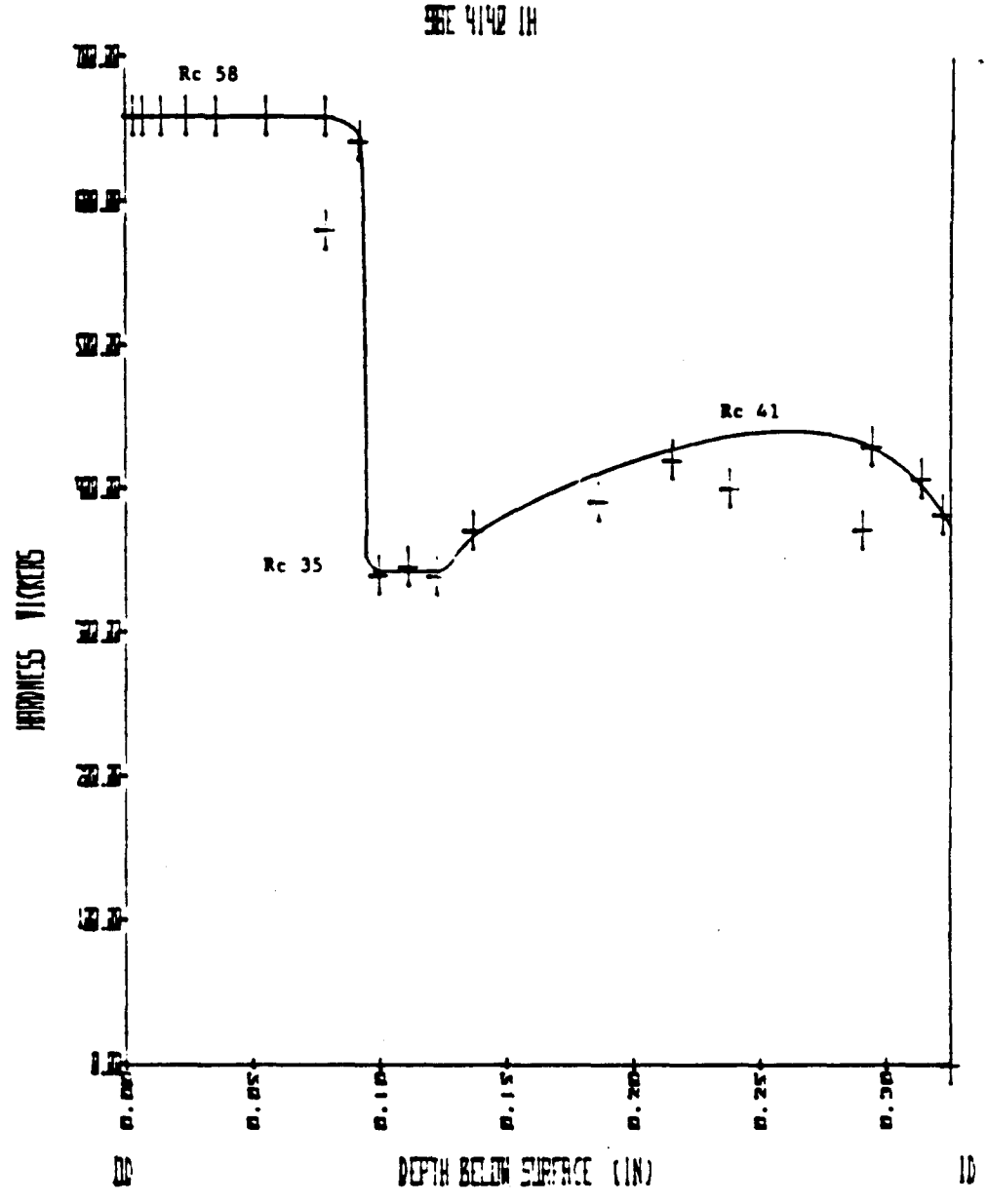

Figure 5-32. Hardness Profile of Induction Hardened 4140 Pin.

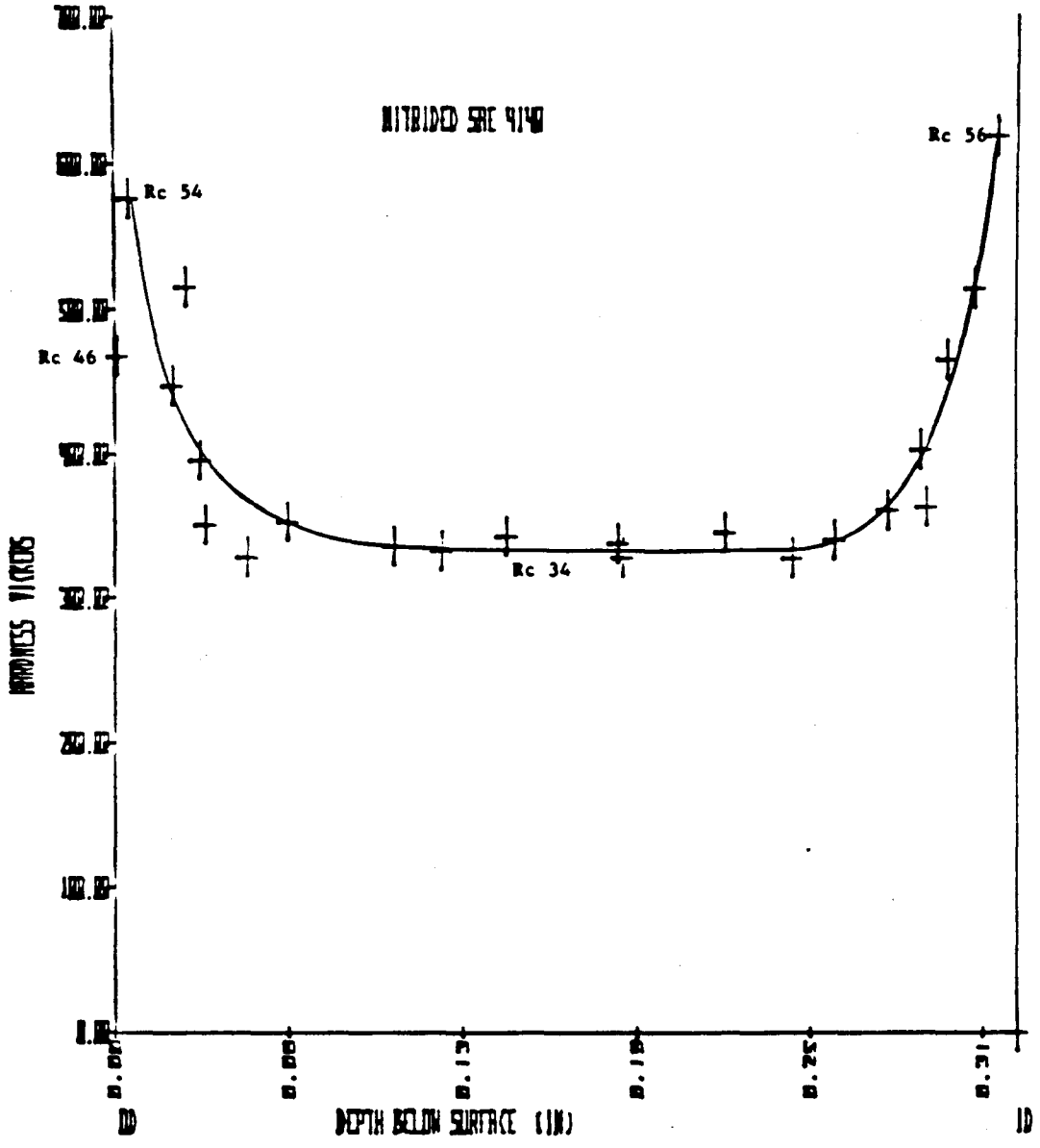

Figure 5-33. Hardness Profile of Nitrided 4140 Pin.

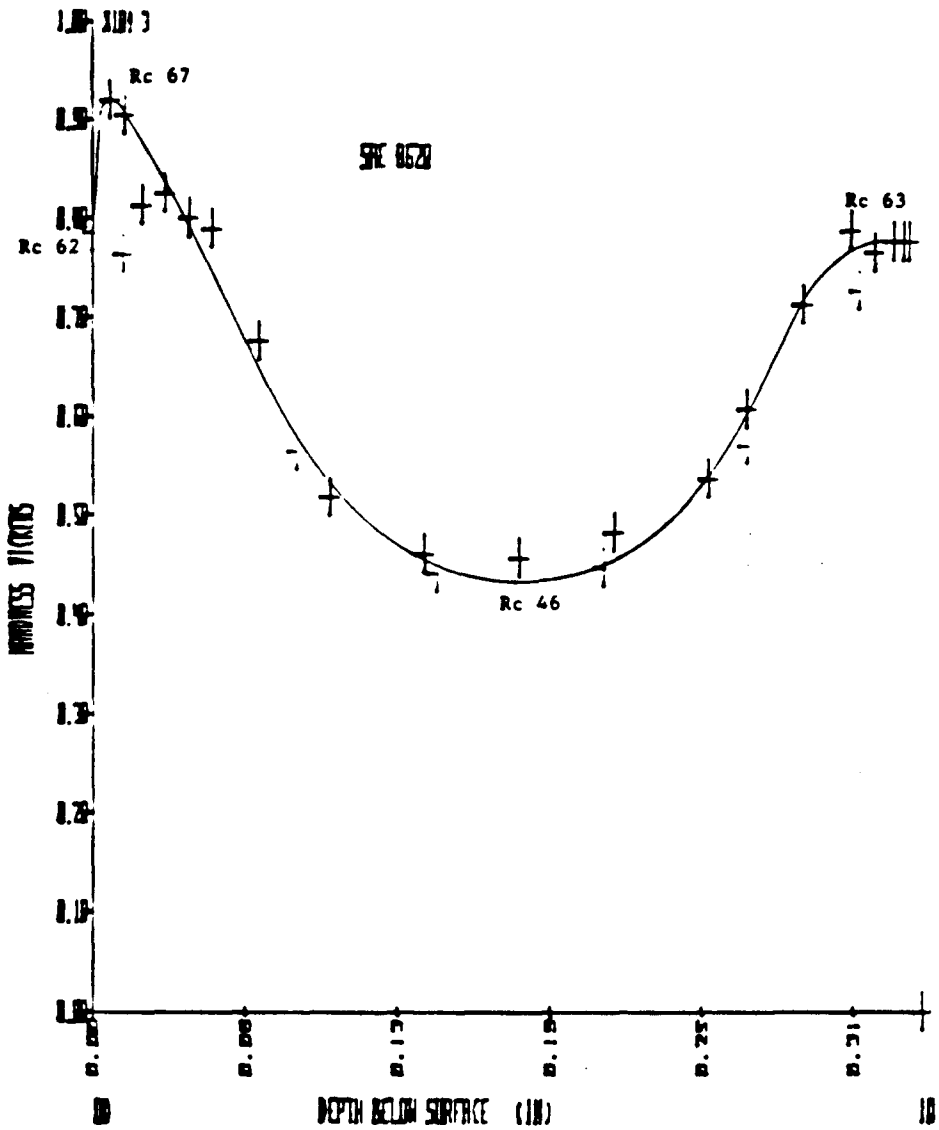

Figure 5-34. Hardness Profile of Carburized 8620 Pin.

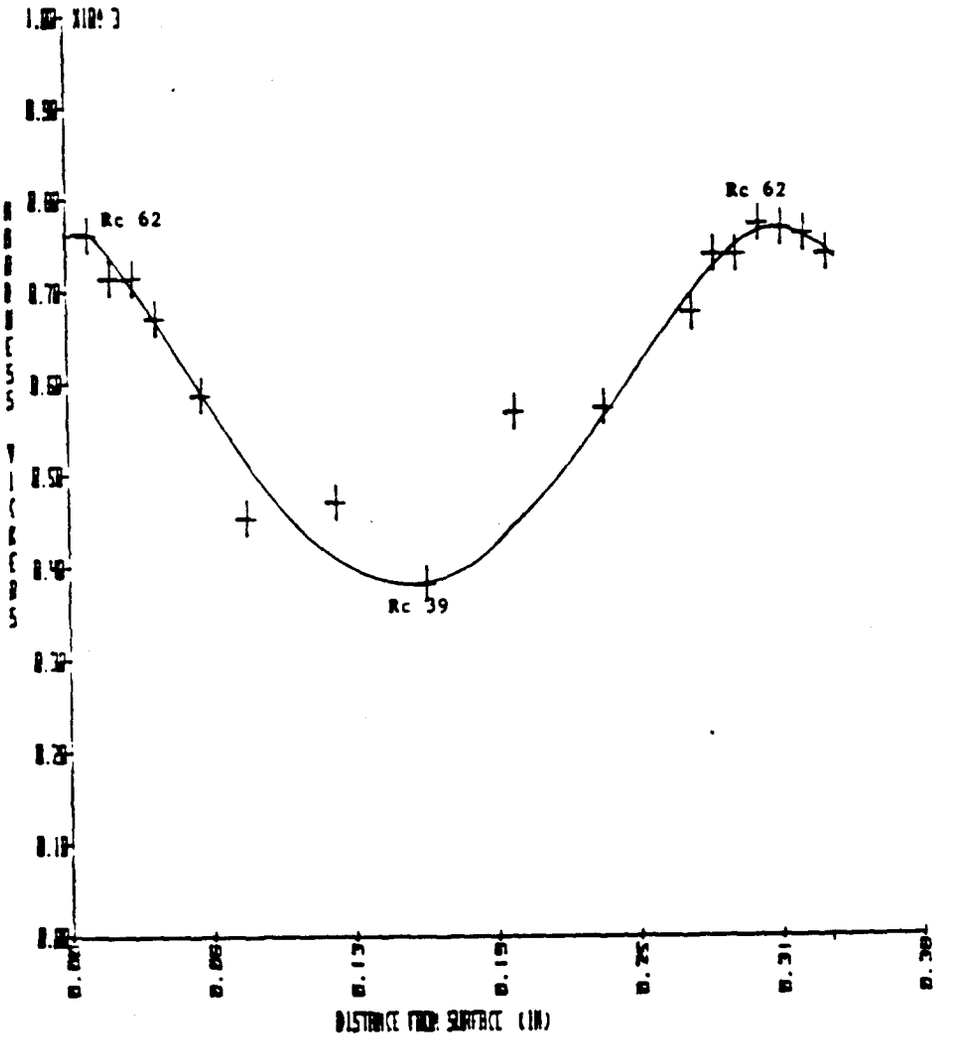

Figure 5-35. Hardness Profile of Carburized 1045 Pin.

the globular oxide type according to the ASTM standard [43]. Some sulfide and alumina inclusions were also observed in some of the steels as listed in Table 5-14. Since all steels have the same degree of cleanliness, inclusions would not be expected to exert a significant role on differences in fatigue behavior.

5.3.4. Surface Residual Stress

The results of surface residual stress measurement on all specimens in both the fatigued and nonfatigued condition are listed in Table 5-15.

5.3.4.1. Stress Shot Peened 8650H. Measurements on two specimens of 8650H pins in the nonfatigued condition indicate an average residual stress of -175 ksi and -165 respectively. No significant changes in the residual 30 stress values were observed when the bar was rotated 90 percent and 180 percent relative to the point of first measurement. This indicates that the peening was uniform around the entire surface of the pins even though this was accomplished manually. The magnitude of residual stress measured is fairly close to the estimated maximum residual stress of -212 ksi which should lie beneath the surface within the peened layer. A bar that has been fatigued at the maximum bending stress of 223 ksi for 509,180 cycles indicates a sharp drop in the residual stress from as high as -196 ksi (measured at about 2 inches from the fracture surface) to -60 ksi (measured at about 1 inch from the fracture surface). This indicates that residual stress relaxation occurred during the fatigue process but this is not extensive enough and the residual remains compressive even after the pin fractured.

5.3.4.2. Stress Shot Peened 4340. The surface residual stress on the stress shot peened 4340 steel was measured as -170 ksi in the nonfatigued condition. A pin fatigued at a maximum bending stress of 173 ksi for 206,260 cycles has a similar magnitude of surface residual stress when measured at 2 inches from the fracture surface. This drops to -105 ksi at about 3 inches and -60 ksi at 1 inch from the fracture surface edge. This again indicates that residual stress relaxation occurred only within approximately 1 inch of the mid position of the pin where the applied stress is maximum at the outer fiber. Outside this region, no apparent residual stress relaxation occurs. This residual stress relaxation would be expected with micro yielding that requires a stress over 50 percent of the engineering yield strength.

5.3.4.3. Induction Hardened 4340 and 4140. The surface residual stress of nonfatigued induction hardened and shot peened 4340 and 4140 pins are about equal in magnitude ranging from -102 to -119 ksi. This is in close agreement with data from Snyder [39] who reported a surface residual stress of -110 ksi on a similarly processed 8650H pin. A 4340 bar fatigued at a maximum bending stress of 209 ksi for 63,530 cycles has a surface residual stress of -20 ksi near the fracture surface. The 4140 pin fatigued

Table 5-14. Inclusion Content of Steels

Steel	Rating
8650H	D2 Heavy and B2 Heavy
4340	D2 Thin and A2 Thin
4140	D2 Thin and B2 Thin
8620	D2 Thin
1045	D2 Thin

Note:

A2 Thin - Sulfide type inclusion with approximate thickness up to 4 microns (0.00016 inch)

B2 Thin - Alumina type inclusion with approximate thickness up to 9 microns (0.00035 inch)

B2 Heavy - Alumina type inclusion with approximate thickness up to 15 microns (0.0006 inch)

D2 Thin - Globular oxide type inclusion with approximate thickness up to 8 microns (0.0003 inch)

D2 Heavy - Globular oxide type inclusion with approximate thickness up to 12 microns (0.0005 inch)

* From "Recommended Practice for Determining the Inclusion Content of Steel", ASTM Standard Designation E45.

Table 5-15. Results of Surface Residual Stress Measurement

Material	Residual Stress, ksi
1. 8650H - nonfatigued	-175[a]
2. 8650H - nonfatigued	-165[a]
3. 8650H - fatigued at o_{max}=223 ksi for 509,180 cycles	-188[a], -60[d]
4. 4340 stress shot peened-nonfatigued	-170[a]
5. 4340 stress shot peened-fatigued at o_{max}=173 ksi for 206,260 cycles	-165[a], -105[b], -72[c], -60[d]
6. 4340 induction hardened-nonfatigued	-112[a]
7. 4340 induction hardened-fatigued at o_{max}=209 ksi for 63,530 cycles	-116[a], -20[d]
8. 4140 induction hardened-nonfatigued	-106[a]
9. 4140 induction hardened-fatigued at o_{max}= 220 ksi for 51,850 cycles	-108[a], -32[d]
10. 4140 nitrided - nonfatigued	-105[a]
11. 4140 nitrided - fatigued at o_{max}=213 ksi for 40,510 cycles	-113[a]
12. 8620 carburized - nonfatigued	-106[a]
13. 8620 carburized - fatigued at o_{max}=181 ksi for 80,110 cycles	-55[d]
14. 1045 carburized - nonfatigued	-41[a]
15. 1045 carburized - fatigued at o_{max}=170 ksi for 8,750 cycles	+10[d]

a - measured at 4 inches from fracture surface
b - measured at $\frac{3}{16}$ inch from fracture surface
c - measured at $\frac{1}{8}$ inch from fracture surface
d - measured at $\frac{1}{16}$ inch from fracture surface

at a maximum bending stress of 220 ksi for 51,850 cycles demonstrates a residual stress of -32 ksi.

5.3.4.4. Nitrided 4140. These pins which have been nitrided and shot peened possess a surface residual stress of -110 ksi in the nonfatigued condition. A fatigued pin which has been tested at 213 ksi maximum bending stress for 40,510 cycles, shows a decay in residual stress to -54 ksi near the fracture surface.

5.3.4.5. Carburized 8620. The residual stress on these pins was measured at -106 ksi. When fatigued at a maximum bending stress of 181 ksi for 80,110 cycles, a low -60 ksi was measured near the fracture surface.

5.3.4.6. Carburized 1045. These pins which have not been peened have a very low surface residual stress of -52 ksi in the nonfatigued condition. When fatigued at a maximum bending stress of 170 ksi for 8,750 cycles, a tensile residual stress of 10 ksi was measured. This indicates complete residual stress relaxation has occurred during the fatiguing process.

5.3.5. Metallographic Results

The induction hardened 8650H, 4340 and 4140 steels have a slightly self tempered fine martensite microstructure in the case shown in Figure 5-36. The core is primarily tempered martensite with about 10 percent globular ferrite as shown in Figure 5-37.

Although the 4140 steel was double-stage gas nitrided, it has a thin white layer of Fe_2N of 0.0001 to 0.0002 inch thick on the outer surface. Below the white layer dispersed plate like iron nitride are present in a shallow iron nitride case together with a fine martensite structure as illustrated in Figure 5-38. The inner surface has a thicker white layer of 0.0002 to 0.0003 inch thick. The core is primarily tempered martensite with about 10 percent ferrite.

The carburized 8620 steel demonstrates a slightly tempered, high carbon martensite with about 10 percent retained austenite in the case at both the outer and inner surfaces. Close to the surface, the amount of retained austenite disappears and the stucture is completely tempered martensite as illustrated in Figure 5-39. The core consists of about 15 percent pearlite and 10 percent ferrite in a tempered martensite matrix as indicated in Figure 5-40.

The carburized 1045 steel has tempered martensite microstructure in the case. In the central portion of the core is 50 percent pearlite with about 3 percent ferrite. No pearlite is present in areas closer to the case.

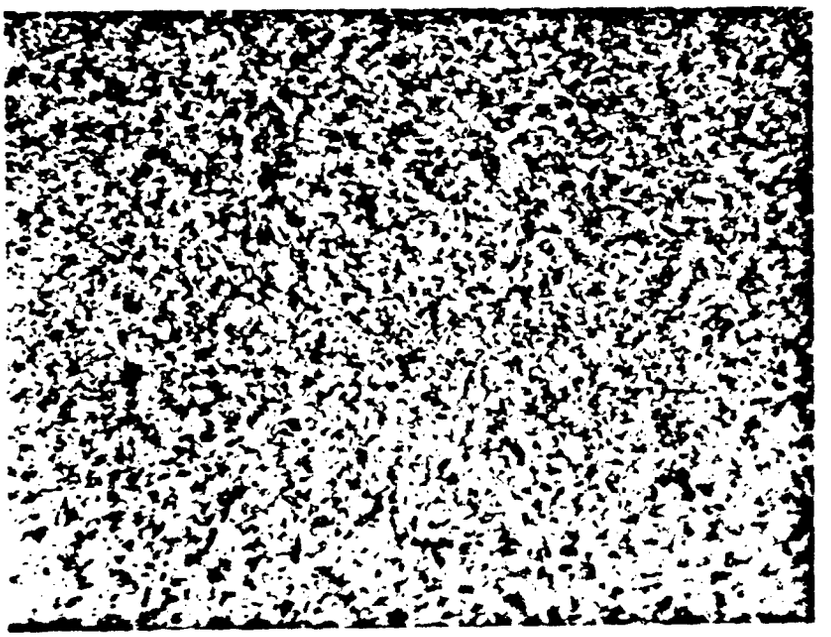

Figure 5-36. Case Microstructure of Induction Hardened 8650H Steel. Structure: Self Tempered Fine Martensite. 2% Nital Etched, 600 X

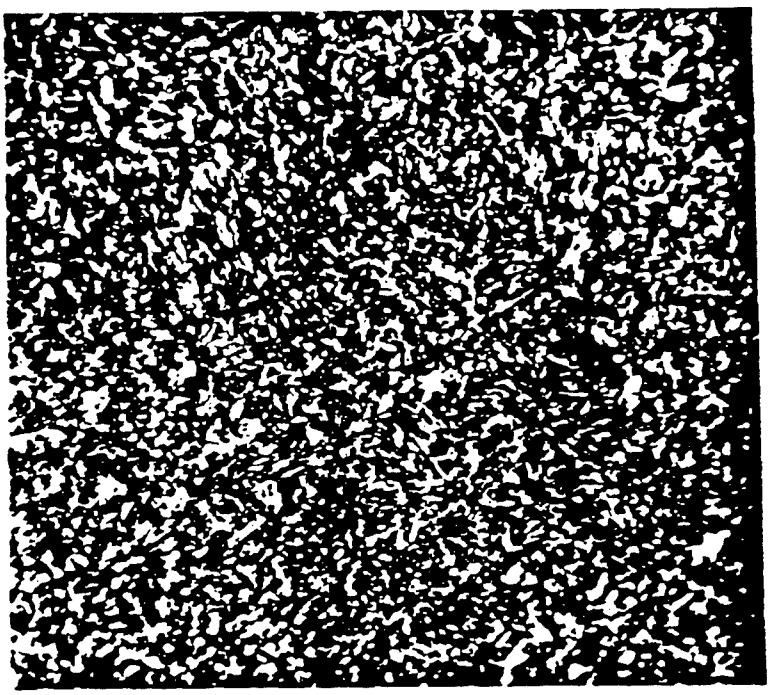

Figure 5-37. Core Microstructure of Induction Hardened 8650H Steel: Tempered Martensite and Ferrite. 2% Nital Etched, 600 X

Figure 5-38. Case Microstructure of Carburized 8620 Pin: Slightly Tempered Martensite and Retained Austenite. 2% Nital Etched, 600 X

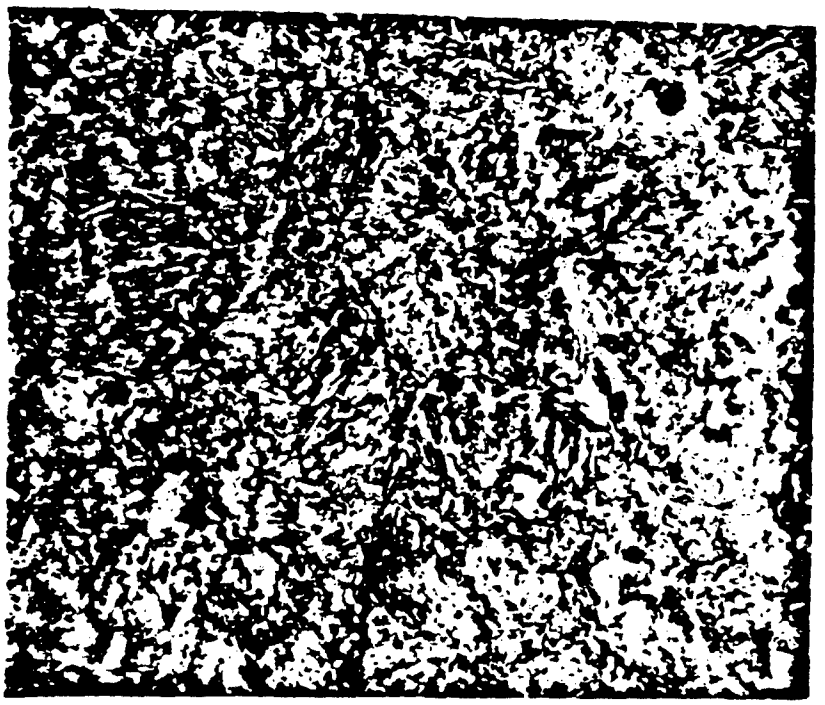

Figure 5-39. Core Microstructure of Carburized 8620 Pin: Tempered Martensite, Pearlite and Ferrite. 2% Nital Etched, 600 X

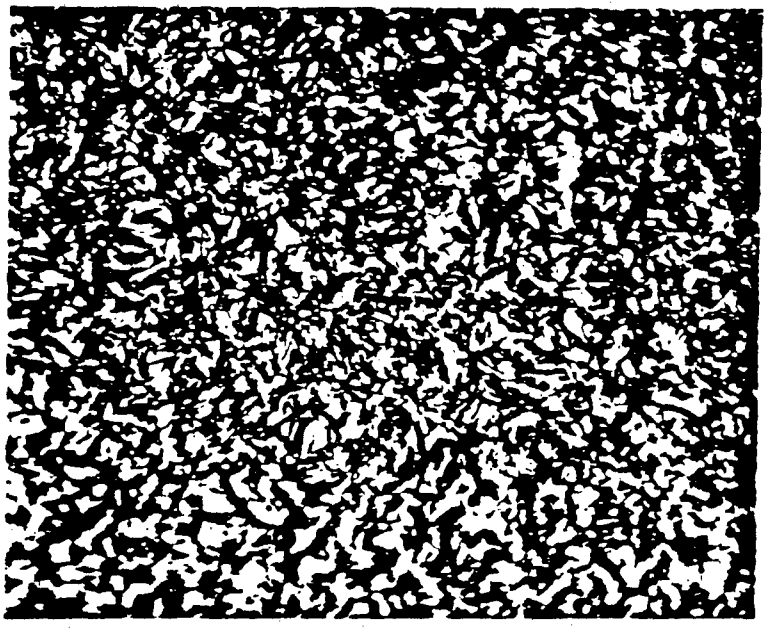

Figure 5-40. Case Microstructure of Carburized 1045 Steel: Tempered Martensite and Retained Austenite. 2% Nital Etched, 600 X

5.3.6. General Discussion

Stress shot peening is the most potent method of improving the fatigue strength of the tank track pins. The stress shot peened 8650H steel pins have a high residual stress that provides these improved fatigue properties. The pins in the as received condition that were conventionally shot peened, have a residual compressive stress of -110 ksi on the surface and an endurance limit of 155 ksi [39]. The stress shot peened 8650H steel pins have a higher compressive residual stress of -175 ksi on the surface and a correspondingly high endurance limit of 198 ksi. The stress shot peened 4340 steel pins did not provide as much improvement in the fatigue strength because of the weakening effect on the inner surface brought about by the larger bore hole size of the pin. As a result, although the outer surface was strengthened by a very high compressive residual stress, the inner surface was subjected to a high tensile stress by the bending and was vulnerable to failure. This effect lowers the endurance limit to 170 ksi that is still higher than the as received pins.

Regardless of the surface hardening methods used, the surface residual stress produced by conventional shot peening is about equal in magnitude and ranges from -102 to -116 ksi. Except for the nitrided 4140 pins, the surface hardness range is small (Rc 58 to 62). The magnitude of residual stress at the surface agrees well with the results of another investigator [31]. The endurance limit ranges from 160 to 175 ksi for the 4140, 4340 and 8620 steel pin in the order of increasing endurance limit. The 1045 steel which was only carburized but not shot peened has a very low surface compressive residual stress of only -41 ksi and consequently, very inferior fatigue strength.

The induction hardened and shot peened 4340 and 4140 steel pins demonstrate the effect of changing the material parameter alone on the fatigue properties of the pins. Both pins posses higher fatigue limit than the as received pins. The 4340 steel has a fatigue limit of 170 ksi which is 15 ksi higher than the as received pin. With an endurance limit of 160 ksi, the 4140 steel shows only a slight improvement over the fatigue strength of the as received pin. Both 4340 and 4140 pins experience similar fatigue failure modes with crack origins at the outer surface at high applied stress of approximately 180 ksi, and crack origins at the inner surface at bending stresses below 180 ksi.

When the only variable considered is the type of steel, as in the case of induction hardened 8650H, 4340 and 4140 steels, the 4340 pins illustrates its advantage. The 4340 pins which have the greatest ductility when tested, as indicated by the fracture surface, show the highest fatigue limit in the group. Its ability to accommodate flaws and thus reduce the stress concentration at these points was cited the possible reason for the better fatigue strength. Comparison between 8650H and 4340 and 4140 pins

also involves an additional size factor. An oversize bore of 4340 and 4140 pins by only 0.1 inch in diameter apparently makes the inner surface vulnerable to failure at certain bending stress levels. At a calculated bending stress level of 200 ksi, the tensile stress at the inner surface is 16 ksi larger than the stress at the inner surface of 8650H psi. When the outer surface is strengthened by a very high compressive residual stress, as in the case of stress shot peened 4340 pins, failure occurs only at the inner surface. However, when the inner surface is strengthened by the carburizing and nitriding treatments, as in 8620 and 4140 steels, no such failure was observed.

The carburizing treatment of 8620 steel pins produces the highest surface and core hardness of Rc 62 and Rc 46 respectively. The case has a tempered martensite microstructure with a hardness as high as Rc 67 near the surface. Finishing the carburized pins with shot peening increases the surface residual stress to about -110 ksi. As a result, this steel possesses the second highest fatigue limit of 175 ksi after the stress shot peened 8650H pins.

The nitriding process on the other hand, did not produce the expected high surface hardness. With a spotty low hardness of Rc 46 on the surface and Rc 35 in the core, the 4140 steel has an endurance limit of only 160 ksi. Despite the two-stage gas nitriding process given to this steel, white layers in the outer and inner surfaces still exist. Consequently, this results in a low endurance limit.

THIS PAGE INTENTIONALLY LEFT BLANK

LIST OF REFERENCES

1
Fatigue Durability of Carburized Steel, American Society for Metals, Cleveland, Ohio, 1957, Lectures Presented by General Motors Corp. Researchers at the 38th National Metals Congress, Oct. 8-12, 1956, Cleveland, Ohio.

2
Koistinen, D. P. and Marburger, R. E., "Internal Stresses Induced By Phase Transformations,", Proc. Symposium Internal Stresses and Fatigue in Metals, Detriot and Warren, Michigan, 1958, Elsevier Publishing Co., New York, N.Y., 1969, pp 110-111.

3
Boegehold, A. L., Metal Progress, March 1950.

4
Straub and May, "Stress Peening," Iron Age, April 21, 1949, pp 67-70.

5
Mattson, R. L. and Roberts, J. G., "Effect of Residual Stresses Induced by Strain Peening Upon Fatigue Strength," Internal Stresses and Fatigue in Metals, Elsevier Publishing Co., New York, 1960, pp 337-360.

6
Moore, H. F., "Strengthening Metals by Shot Peening", Shot Peening, 9th Ed., 1977, Publication by Wheelabrator-Frye, Inc., Mishikawa, Indiana, p 79.

7
Almen J. O. and Black, P. H., "Residual Stresses and Fatigue in Metals", McGraw Hill Book Co., Inc., New York, N.Y., Chapters 5 and 6.

8
Wulpi, D. J. ed, "How Components Fail", ASM, Metals Parks, Ohio, 1966.

9
Dolan, T. J. "Physical Properties," in ASME Handbook, Metals Engineering Design, O.J. Horger, ed., McGraw Hill, New York, 1953.

10
Rally, F. C. and Sinclair, G. M., "Influence of Strain Aging On The Shape of S-N Diagram", Department of Theoretical and Applied Mechanics, University of Illinois, Urbana, Ill., 1955.

LIST OF REFERENCES (Continued)

11
Lipsitt, H. A. and Horne, G. T., "The Fatigue Behavior Of Decarburized Steels", Proc. ASTM, Vol. 57, 1957, pp 587-600.

12
Orawan, E., Proc. Roy. Soc. (London), Vol. 171A, pp 79-106, 1939.

13
Wood, W. A., Bull. Inst. Metals, Vol. 3, pp 5-6, Sept. 1955.

14
Cottrell, A. H. and Hull, D., Proc. Roy. Soc. (London) Vol. 242A, pp 211-213, 1957.

15
Mott, N. F., Acta Met., Vol. 6, pp 195-197, 1958.

16
Frost, N. E. March, K. J. and Pook, Oxford University Press, London, 1974.

17
Breen, D. H. and Wene, E. M., "Fatigue In Machine Structures - Ground Vehicles," in Fatigue and Microstructure, ASM, Ohio, 1979.

18
Parker, E. R., "Brittle Behavior of Engineering Structures", Wiley & Sons, New York, 1957.

19
Dieter, G. E., "Mechanical Metallurgy", McGraw Hill, New York, 1961, Chapter 12.

20
Madayag, A. F. "Metal Fatigue: Theory and Design" John Wiley & Sons, New York, 1969, Chapters 1 and 3.

21
Fluck, P. G., "The Influence of Surface On the Fatigue Life and Scatter of Test Results of Two Steels," Proc. ASTM, Vol. 51, 1951, p 584.

22
Forrest, G., "The Effect On Fatigue of Notches, Surface Finish, etc.," The Fatigue of Metals, The Inst. of Metallurgists, London, England (Lectures at Refresher Course), 1955, p 69.

LIST OF REFERENCES (Continued)

23
Hempel, M.R., "Surface Condition and Fatigue Strength" Internal Stresses and Fatigue in Metals, Proc. of Symposium on Internal Stresses and Fatigue in Metals, Detroit and Warren, Michigan, 1958, Elsevier Publishing Co., New York, N.Y., pp 312-313.

24
Vishnevsky, C., Bertolino, N. F., Wallace J. F. and Briggs, C. W., "Effect of Surface Discontinuities on Fatigue Properties of Cast Steel Sections," ASME Publication 67-WA/MET-17, New York, N.Y., 1967.

25
Das, G.,"Influence of Processing variables on the Fatigue Behavior of Cast Steel," M. S. Thesis, Case Western Reserve University, Cleveland, Ohio, Sept. 1968.

26
Kotovich, C. S., Tager S. and Wallace, J. F., "Influence of Surface Condition on Mechanical Behavior of High Strength Steel Casting," Report
Prepared Under Army Materials and Mechanics Center, Contract No. AMMRC CR 70-07, Dec. 1969.

27
Kotovich, C. S., "Influence of Mold Steel Interactions on Casting Surface Quality and Properties," Ph.D. Thesis, Case Western Reserve University, Cleveland, Ohio, August 1973.

28
Beebe, W. M. "A Simplified Theory for Dynamic Failure in Solid Materials," Mechanical Prestressing, SAE Report SP-181, Biennal MeeTing May 16-18, 1960, New York, N.Y., p 2.

29
Jackson L. R. and Pochapsky, T. E.,"The Effect of Composition on the Fatigue Strength of Decarburized Steel," Trans, ASM, Vol. 39, 1947, pp 45-60.

30
Harris, W. J., "The Influence of Decarburization on the Fatigue Behavior of Steel Bolts," Report on Work Carried Out by Hawker Siddeley Aviation Ltd. Under British Ministry of Aviation Contract, 1965.

31
Metals Handbook, 8th Edition, Vol.1, American Society for Metals, Metals Park, Ohio, 1961, p 221.

32
Brookman J. G. and Kiddle, L.,"The Prevention of Fatigue Failure in Metal Parts by Shot Peening," The Failure of Metals by Fatigue, Proc. Symposium University of Melbourne Australia, Melbourne University Press, 1946, pp 395-396.

33
Shot Peening Applications, Publication by Metals Improvement Co., 5th Ed.

34
Straub, J.C., "Choosing the Optimum Method Intensity Coverage of Shot Peening," Mechanical Prestressing, SAE Report SP-181, 1960, p 9-10.

35
Borik, F., Chapman R. D. and Jominy, W. E., "The Effect of Percent Tempered Martensite on Endurance Limit," Trans. of the ASM, Vol. 50, 1958, pp 242-257.

36
Hubbell H. and Pearson, P. K., "Non Metallic Inclusions and Fatigue Under Very High Stress Conditions," Quality Requirements of Super Duty Steels, Vol. 3, Interscience, 1959.

37
Oreilly, P. J., DMIC Report No. 200 on High Strength Steels, 1964.

38
Cummins, H. N., Stulen, F. B. and Schulte, W. C., "Relations of Inclusions in High Strength Steels," ASTM Proc., Vol. 58, 1958, p 505.

39
Snyder, J. T. and Wallace, J. F., "Reheat Treatment and Reclamation of Used Tank Track Pins," unpublished, 1984.

40
Nelson, D. V., Ricklefs R. E. and Evans, W. P., "The Role of Residual Stresses in Increasing Long-Life Fatigue Strength of Notched Machine Members," Achievement of High Fatigue Resistance In Metals and Alloys, ASTM STP 467, American Society For Testing and Materials, 1970, pp 228-253.

41
"Shot Peening of Metal Parts," Military Specification MIL-S-13165B, 1979.

42
Publication by American Analytical Corp., Grafton, Ohio.

43
"Recommended Practice for Determining the Inclusion Content of Steel," ASTM Standard Designation E45, American Society for Testing and Materials, Philadelphia.

THIS PAGE INTENTIONALLY LEFT BLANK

DISTRIBUTION LIST

	Copies
Commander US Army Tank-Automotive Command ATTN: DRSTA-RCKT (Mr. Joe Fix) 6300 East 11 Mile Road Warren, MI 48397-5000	10
Commander US Army Tank-Automotive Command ATTN: AMSTA-TSL (Technical Library) Warren, MI 48397-5000	14
Commander Defense Technical Information Center Bldg. 5, Cameron Station ATTN: DDAC Alexandria, VA 22314	12
Commander US Army Tank-Automotive Command ATTN: DRSTA-IRRD 6300 East 11 Mile Road Warren, MI 48397-5000	1
Commander US Army Tank-Automotive Command ATTN: ACO 6300 East 11 Mile Road Warren, MI 48397-5000	1
Commander US Army Tank-Automotive Command ATTN: DRSTA-TSE 6300 East 11 Mile Road Warren, MI 48397-5000	1